2014

Design of A New Membrane Stretching Device

Yiran Shao
Lehigh University

DESIGN OF A NEW MEMBRANE STRETCHING DEVICE

by

Yiran Shao

A Thesis

Presented to the Graduate and Research Committee of

Lehigh University

in Candidacy for the Degree of

Master of Science

in

Mechanical Engineering and Mechanics

Lehigh University

July, 2014

This thesis is accepted and approved in partial fulfillment of the requirements for the Master of Science.

_____

Date

_____

Thesis Advisor

_____

Chairperson of Department

ACKNOWLEDGMENTS

First, I would like to thank my advisor, Professor Yaling Liu. Without his encouragement, comments, and guidance during my design, I could not finish my thesis. Secondly, I want to give my appreciation to my Lab mates, especially Doruk Yunus, Ran He, Christopher Uhl and Wentao Shi. They give me a lot of advices to help me with my design. Their enthusiasm, concentration and patience on research affect me a lot.

During my Master's study at Lehigh University, I deeply enjoyed my courses and lab work. I have learned not only the knowledge, but also the purest attitude to study from faculty and staff. I will keep this deep in my mind to guide my future work.

Finally, I would like to express my deepest appreciation to my parents and friends for their endless support. I want to thank my girlfriend, but I do not have any.

Table of Contents

LIST OF TABLES

LIST OF FIGURES

Abstract

DESIGN OF A NEW MEMBRANE STRETCHING DEVICE

Yiran Shao

Lehigh University, 2014

Director: Dr. Yaling Liu

Cell stretching device has been applied into the lab use for many years to help researchers study about the behavior of cells during the stretching process. Because the cell responses to the different mechanical stimuli, especially in the case of disease, the cell stretching device is a necessary tool to study the cell behavior in a controlled environment. However existing devices have limitations, such as too big to fit the culture chamber, unable to be observed during the stretching process and too expensive to fabricate. In this thesis, a new cell stretcher is designed to resolve these limitations. Many typical cell stretching devices only work under simple conditions. For instance they can only apply the strain on the cell in uniaxial or equibiaxial directions. On the other hand the environment of cells' survival is varying. Many new cell stretchers have been developed, which have the same property that cells can be stretched via the radical deformation of the elastomeric membrane.

The aim of this new design is to create a cell stretching device that fits in general lab conditions. This device is designed to fit on a microscope to observe, as well as in the incubator. In addition, two small step motors are used to control the strain, adjust the frequency, and maintain the stability precisely. Problems such as the culture media leakage and the membrane breakage are solved by the usage of multiple materials for both the cell

stretcher and the membrane. Based on the experimental results, this device can satisfy the requirements of target users with a reduced manufacturing cost. In the future, an auto-focus tracking function will be developed to allow real time observation of the cells' behavior.

Chapter 1. Introduction

1.1 Background

A variety of activities and functions of the cells are affected by mechanical stimuli which can be divided into the three types: tension, compression and shear (Fig.1). Depending on the type of the mechanical force and the rates at which the force is applied, the response of cells is different [1].

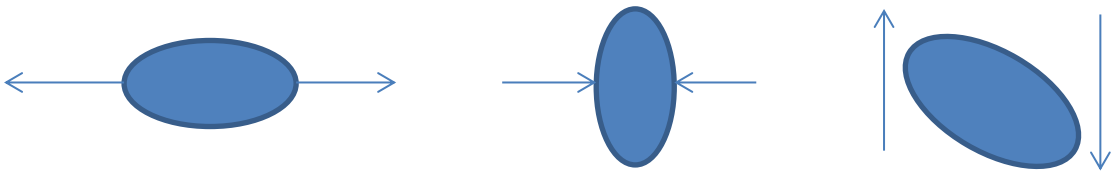

Figure 1: Schematics of different mechanical forces applied on cells

The interaction between cells and their environments, such as changes in adhesion, proliferation, locomotion, morphology, and synthetic profile [2], is based on the mechanical stress which plays an important role in the body. Many types of cells, such as those in muscles, hearts and cardiovascular systems, lungs, connective tissues, skins and bones [1], are affected by the applied force.

Arteries and cardiovascular muscle cells are commonly chosen for the research purpose, since they are constantly strained by the force generated from the blood pressure [3]. It is found that the apoptosis, proliferation, and migration of vascular cells, are all moderated by the cyclic mechanical stretch [3].

Using muscular tissues is another choice for this kind of researches, due to their regular

reactions to the mechanical stresses. The muscular tissue is stretched routinely during daily events from which the muscles undergo extreme stress. Thus, the mass and strength of muscles can change rapidly [4]. The muscles will atrophy without this stress. Contrarily, when this kind of stresses is induced at a certain amount and frequency, it improves the strength and mass of the muscle. It is reported that decrease in mechanical loading will result in the atrophy of muscles [4]. Since the exercise and mechanical stress play important roles on muscle cells. It is crucial to understand physical forces and their effects on the cell.

Among various experimentations, reorientation or realignment of cells are observed when the mechanical force is induced, as well as their functions and activities, such as proliferation, morphology, and differentiation, will change [1]. These findings demonstrate the effects of the mechanical stimuli on the behavior of cells.

Furthermore, another review indicates the mechanical stress applied on the skin will enhance the dermal healing [5, 6]. Several studies have demonstrated that cells will proliferate in the epidermis and vascularity in dermis [5, 6], when cyclic stretch is induced on the animal skin. During the healing process, the scar formation occurs. The mechanical environment will largely affect the resulting scar. Therefore, it is necessary to fully understand the response of cells under the mechanical stress, in order to optimum the recovery of the wound healing.

Human musculoskeletal system is also affected by mechanical forces [7]. Every cell and tissue in this system has ability to convert the mechanical stimuli into the biochemical signal [8]. In addition, this system also has great response to tensile forces and compressive stresses. Several findings have implied that osteogenesis can be promoted by the compressive strain on osteoblasts [8]. Based on these findings, musculoskeletal cells and their functions are

affected by different kinds of mechanical stimuli variously. Therefore, useful therapeutic applications will be accomplished, when deep investigation of the response of the musculoskeletal system to different mechanical forces is achieved.

The existence of pulsatile blood flow in the heart causes the heart valve cells to maintain constant mechanical forces. As mentioned before, the process of remodeling and repair of cells occurs under the mechanical environment. This kind of continuous mechanical loads will damage the cells. Meanwhile, such varying loads will be converted into molecular signals for the repair of tissue. Therefore, understanding the mechanism of various mechanical forces' effects on the heart valves cells is a great assistance to the better treatment of heart valve pathologies.

Until now, the mechanical stimulation of cells in vitro has been achieved by the invention of various systems which are driven by electric motors, hydrostatic pressurization, and regulated vacuum pressure [9]. These three major methods are different techniques, but they achieve the same goal of introducing the mechanical stimulation of cells in vitro.

The devices for the cell stretching are divided into three kinds by different power sources, such as electric motors, hydrostatic pressurization, and regulated vacuum pressure. These cell stretching devices have the similar mechanism to induce the mechanical force on cells and tissues, which utilize the deformation of the membrane to apply strains on cells. Therefore, different cells present various statuses such as apoptosis, proliferation, and migration. Actually almost every investigators and scientists use elastomeric membranes (some of them are transparent for the better observation) to culture the cells. After that, this membrane with cultured cells will be placed on the stretching device. The stretching process may last several

hours at the certain level of the strain and frequency. During this process, cells will response to the mechanical stimulation and may have the chance to get deformed after long-time of stretching. On the other category, these stretching devices can be divided into three types based on strain directions which include uniaxial, equi-biaxial and radical. The following section outlines each of these three methods and reviews devices that utilize these methods.

1.2 Uniaxial and equi-biaxial stretching device

Uniaxial stretching devices can apply mechanical forces on the membrane in one direction, which generates only uniaxial strain cells. Figure 2 shows a typical [15].

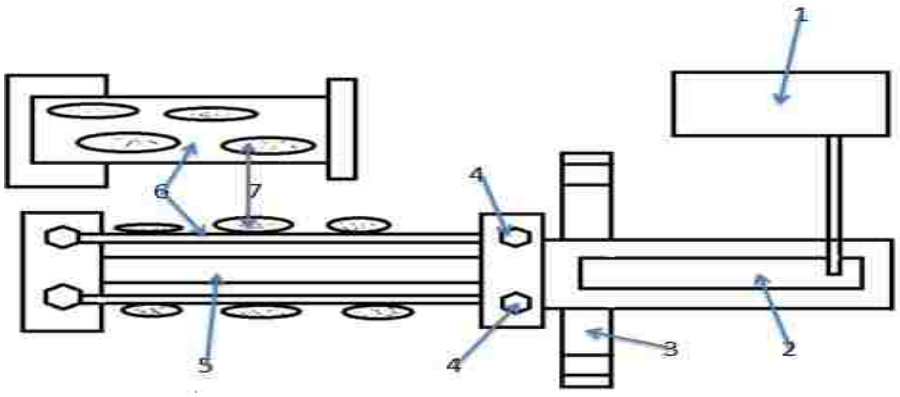

Figure 2: Uniaxial stretching device: 1- Microprocessor-controlled mechanical pump; 2- Fluid reservoir; 3- Gas permeable membrane; 4- Removable support pins; 5- Ram; 6- Extracellular matrix-coated elastic silicon strips; 7- Cells (this figure is re-drawed based on the original figure from [15])

This device uses the hydraulic pressure to apply forces on the membrane to stretch cells linearly. From the illustration above, the cells are cultured on the silicon strip which is attached to the ram whose left end is fixed while the right one is movable. The right end is attached to the hydraulic compression chamber (fluid reservoir). The function of the gas permeable membrane is to maintain the air condition of cells. The stress of this device is applied from the pressure generated by the pump in the hydraulic compression chamber,

which causes the increasing or decreasing the hydraulic force. Therefore, the membrane can be stretched in one direction cyclically, which is induced by the movement of the ram's right end.

The entire device is too big to anchor in the incubator due to its pump and fluid reservoir. That is the reason why the gas permeable membrane is necessary. Certainly, the cell response can be observed on the microscope. However, only uniaxial stretching is not enough to analysis the cell response since they are affected by three forms of stresses.

The disadvantage of uniaxial devices is obvious from the discussion above. To satisfy the requirements of experimentations, the stretching device with multiple functions is necessary. Here is the introduction of the equi-biaxial stretching device (Fig.3) [3, 16].

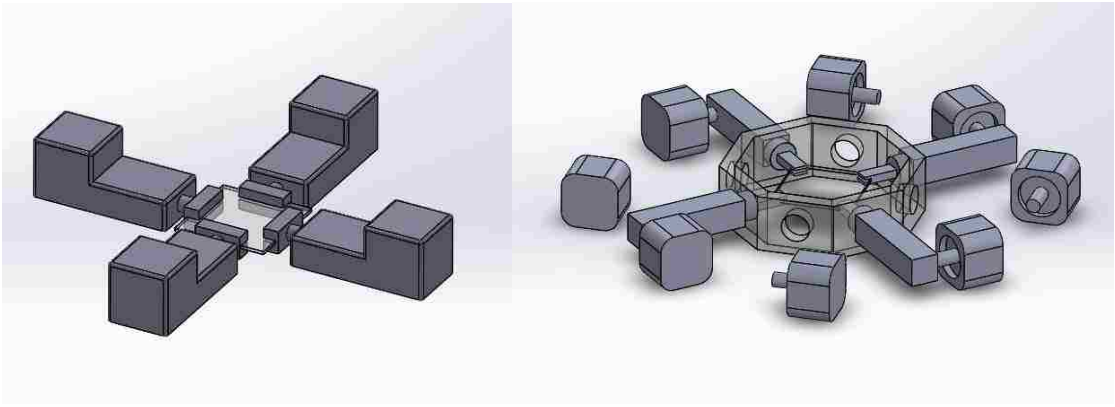

Figure 3: Equi-biaxial stretching device (this figure is re-drawed based on the original figure from [3] and [16])

The above figure shows the schematic view of two customized devices. The left one uses computer operated linear actuators as the power source, while the right one uses eight step motors. This kind of devices has the ability to induce more mechanical stresses on the cells, which is more suitable than the uniaxial stretching devices. The figure of device structure is shown blow (Fig.4) [19].

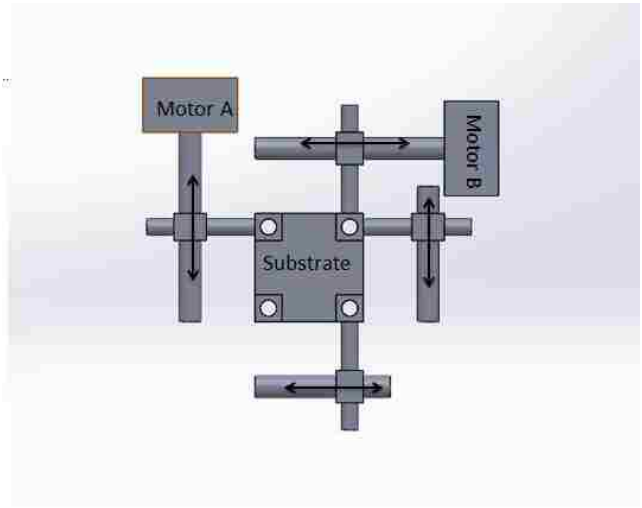

Figure 4: Schematic view of the equi-biaxial stretching device (this figure is re-drawed based on the original figure from [19])

In figure 4, the left lower end of the membrane is fixed on the working plate by nuts and bolts; the two upper ends are connected to two frames that are attached to the threaded rods motivated by motor A. Meanwhile the threaded rods connected with the right two ends are motivated by motor B. Each threaded rod is perpendicular to each other, which means this membrane is stretched in two perpendicular directions. Each step motor is separately controlled by the computer which guarantees different level of the strain applied on the two directions respectively.

The structure of the design in figure 4 is simpler than the two custom devices in figure 3. Comparatively, it is better than the left device (Fig.3) in its less complicated structure. The biggest advantage of the stretching device in figure 4 is the small and simple structure. However cells cannot be stretched uniformly on only two directions, which can be satisfied by the right device (Fig.3) when the eight motors are utilized simultaneously.

Many other equi-biaxial devices will not be introduced. Most of them have the same disadvantages, such as complicated and not stretching uniformly. However a new invented

stretching device (Fig.4) can solve majority of these problems [17].

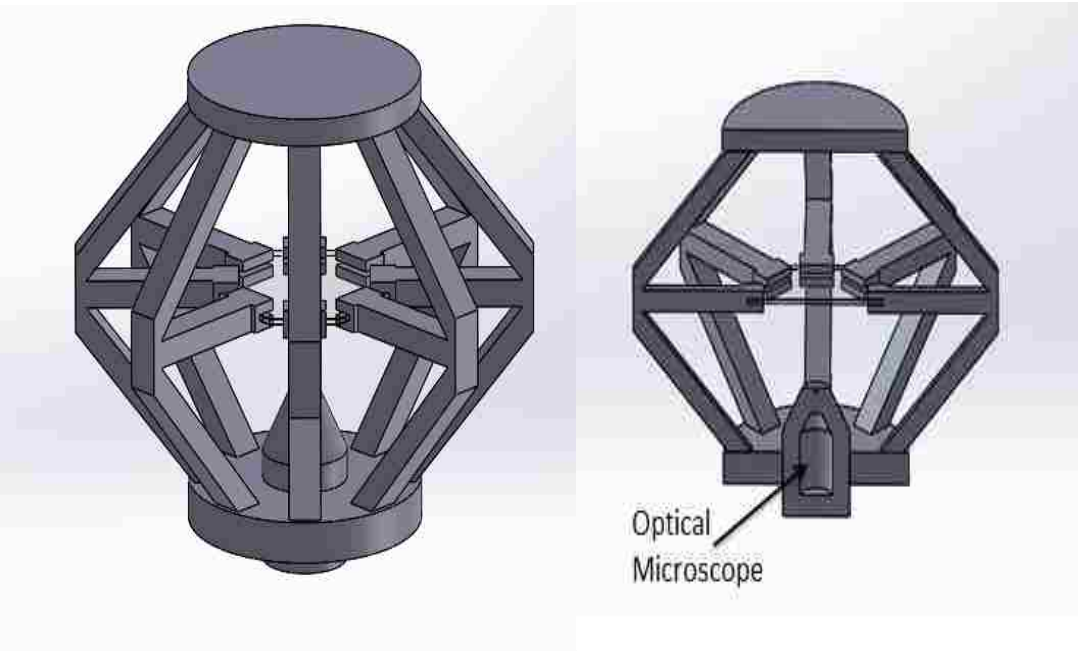

Figure 5: New equi-biaxial Stretcher of a Thin Membrane (this figure is re-drawed based on the original figure from [17])

This figure illustrates the membrane is grasped by eight 3 pronged clasps that are connected to eight V shape beams with eight rods respectively, which maintain the stretching process uniformly. The 8 beams (or legs) mounted to the top and bottom staging platforms. The working process is accomplished by the pressure on the top platform which can be controlled by the machine. The knee of each beam will bend while the pressure is applied on the top that contributes to the centrifugal movement of the eight clasps by which the membrane is stretched.

However, certain flaws cannot be avoided by utilizing this machine. First of all, the membrane cannot be stretched at a cyclical frequency since the membrane moves upward and downward continuously and the lens of optical microscope (Fig.5) is unable to focus on the cultured cells. The cells can be observed only when the membrane is kept at a fixed position during the stretching process. For better observation center hollowed structure of top

platforms is needed in order to provide sufficient light on the membrane. In addition, the cells cannot survive when the device is working, which is shown in Figure 6 [17].

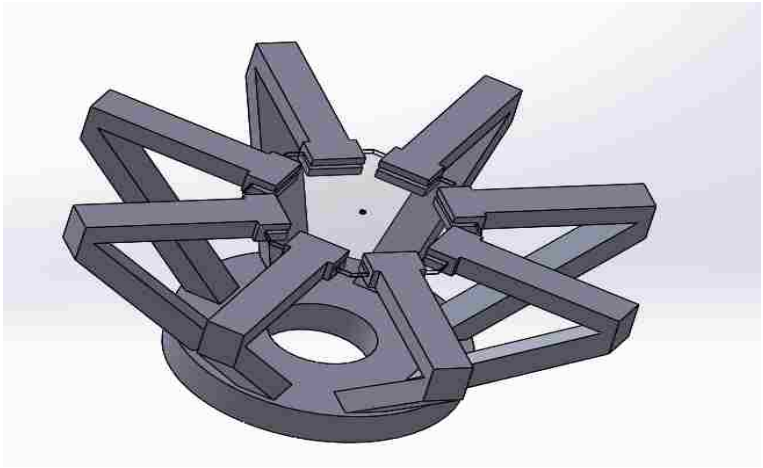

Figure 6: Membrane clasped on the eight clamps (this figure is re-drawed based on the original figure from [17])

To ensure the cells' survival during the stretching process, certain nutrients should be supplied, which are usually resolved in the organic solution. Therefore, a holding structure for the cells' media is necessary on this machine.

From the discussion above, the same disadvantage exists both in uniaxial and equi-biaxial stretching devices that is the inconveniency of assembling and dismantling the membrane. Bolts, nuts or clasps, which are unfriendly for the user in the large amount of ends attached to the stress source, are usually used to assemble the membrane. Investigators should pay more attention to this process in case of damaging the cells. Therefore, various flaws of the uniaxial and equi-biaxial stretching devices underlie the invention of radical stretching devices.

1.3 Radical stretching devices

Radical stretching devices generally use a solid cylinder to push the membrane after the

membrane is fixed on the platform. To understand this procedure directly, figure 7 is shown below [18].

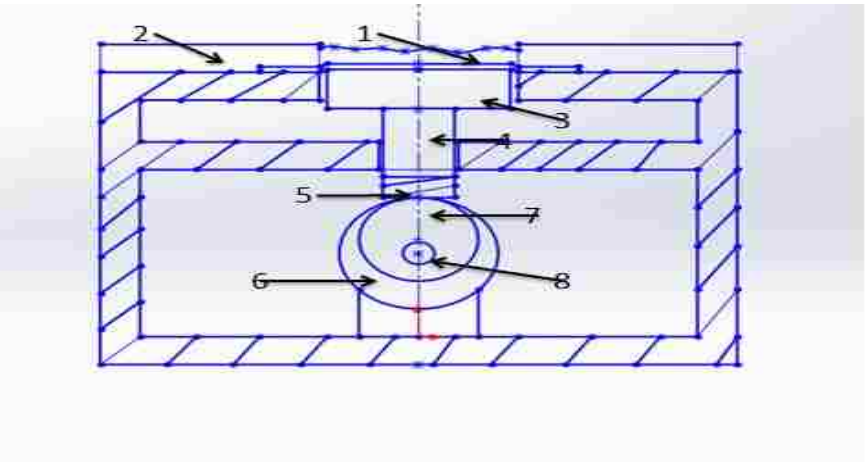

Figure 7: Working process of the radical device: 1- Media; 2- Fix cup; 3- Applicator; 4- Rod; 5-Spring; 6- Electric motor; 7- Cam; 8- Axis (this figure is re-drawed based on the original figure from [18])

This device uses an electric motor to actuate a cam (Fig.7-7), which rotates around the axis (Fig.7-8). The rotation of the cam results in the contact of the applicator (Fig.7-23 and the rod that enables the vertical movement. The circular silicone substrate, seeded with cells is placed right above the applicator and attached firmly to prevent the leakage by utilizing the fix cup (Fig.7-2) which is assembled by the screw bolts. To guarantee the survival of cells during the working process, the media poured in the center hole of the fix cup. The applicator deforms the silicone substrate radically when the motor drives the cam and moves the rod upward. At the end of the upward stroke, the spring (Fig.7-5) will help to the rod from the applicator and return to the original position. Thereby, the cells can be stretched cyclically through the repetitive movement by such a mechanism.

Certainly, depending on various power sources and different working mechanisms, different devices have variety of structures. The following session is about the devices with

various mechanical systems.

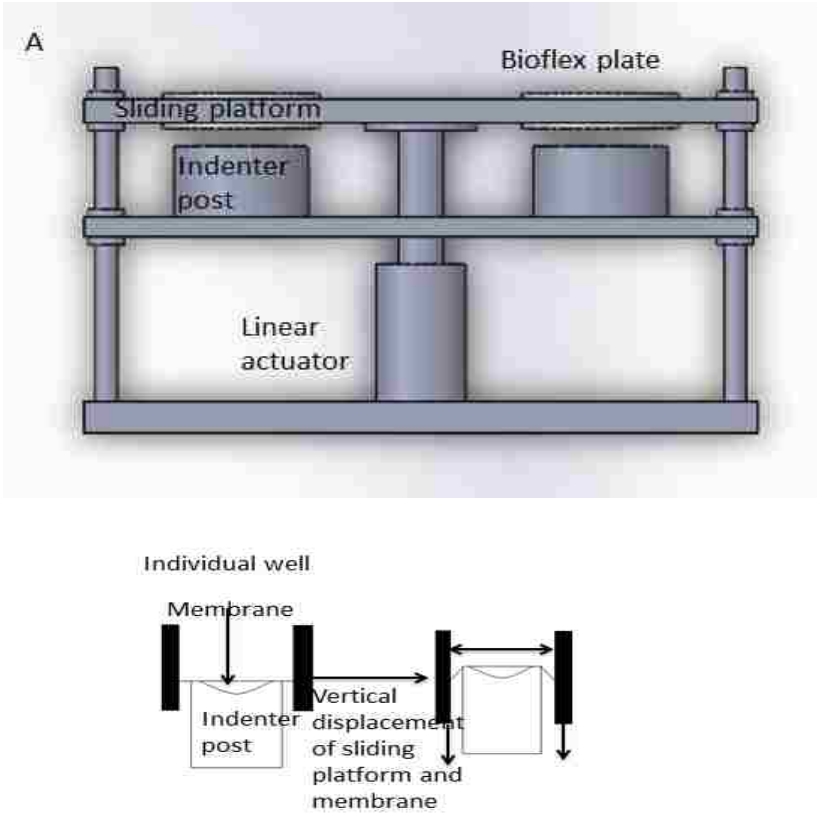

Figure 8: Schematic views of the radical stretching device: (A) Side view of the whole device; (b) Expansion of Membrane (this figure is re-drawed based on the original figure from [13])

In figure.8 [13], two bioflex plates (Flexcell Int, Hillsboro, NC) with six wells and transparent membrane are anchored in the sliding platform whose vertical displacement is controlled by a linear actuator, which is mounted on the bottom of the device (Fig.8-a). The indenter post is directly mounted on a stationary platform below each well that has the lubricant on it to decrease the friction. When the actuator drives the sliding platform to move downward, the expansion of the membrane will occur radically. When the platform returns to the original position, the deformed membrane will recover to the initial condition. Based on the structure of this device, no matter whether the indenter post is hollow or not, the cells cannot be observed by the microscope directly.

The bioflex plates mentioned above is originally used for a custom device--the Flexcell tension system. Different from the device above, the Flexcell tension system uses the vacuum pump as the power source (Fig.9) [12].

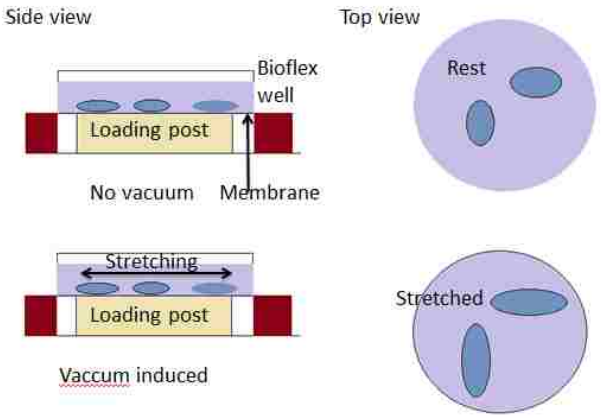

Figure 9: Vacuum pressure Flexcell stretching device (this figure is re-drawed based on the original figure from [12])

The right of figure 9 illustrates the working process of the Flexcell. Similarly, cells are cultured on an elastomeric substrate which will be anchored directly above a loading post. The strain and the frequency of vacuum are controlled by the computer. When the vacuum is induced, the surrounding parts of the substrate will move downward. Therefore, the middle region of the substrate will be stretched. After applying and removing the vacuum repetitively, the cyclic stretching on the cells can be achieved. During the working process, the base plate can be placed in the incubator to supply a suitable environment for the cells. However, this process cannot be observed by the microscope directly either, as the loading post is not transparent enough to ensure the penetration of the light. To solve this issue, this company provides another device whose working mechanism is similar to the Flexcell tension system (Fig.10) [12].

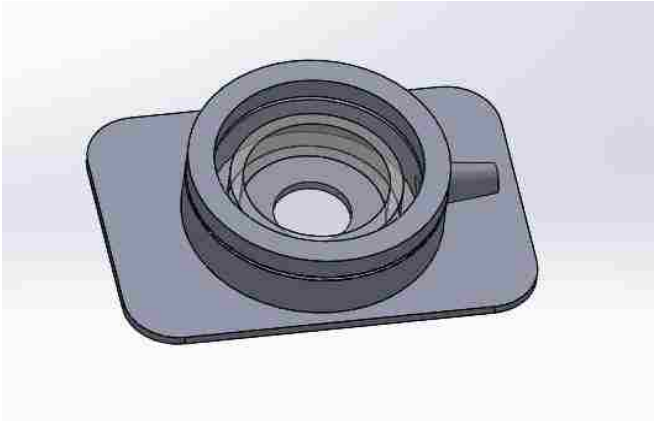

Figure 10: Schematic view of the Flexcell® StageFlexer® for the microscope (this figure is re-drawed based on the original figure from [12])

This device use four screw bolts to maintain the air tight. The hollowed and transparent middle part of loading post allows the light to penetrate through. The device has a simple structure and smallest size among existing devices. Nevertheless, the whole system is still too big to set up easily, because of the large dimension of the vacuum pump.

Since the big size of the devices with the linear actuator and vacuum pump causes inconvenient for the assembling, observation, and movement, using motors is the better selection for the invention of a new stretching device. Motors are considered to have a small size and being controlled by the computer easily and accurately. The following part is the introduction of the radical device utilizing motors as the power source.

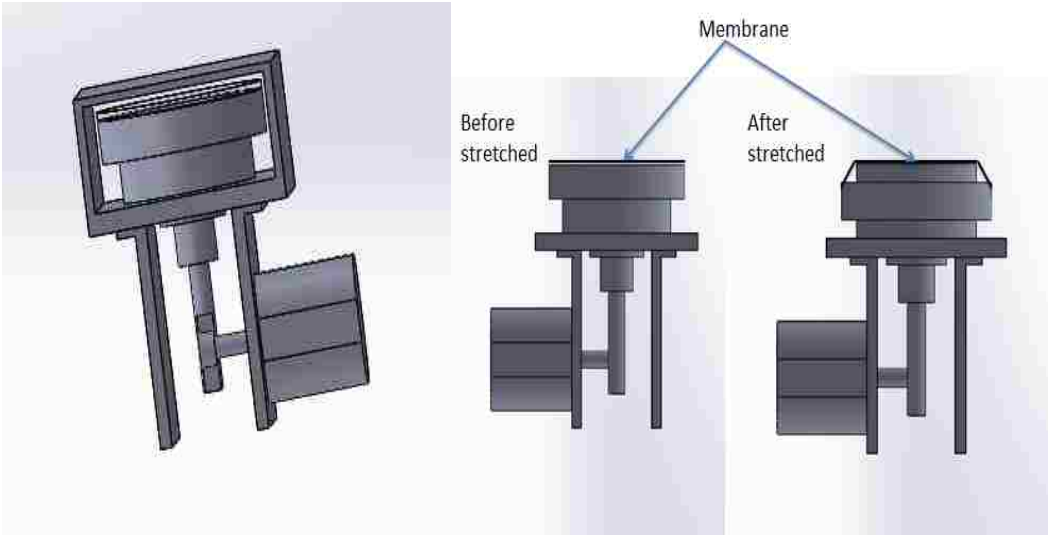

Figure 11: Schematic view of the stretching device with the step motor (left); schematic view of the membrane deformation (right) (this figure is re-drawed based on the original figure from [14])

In figure.11 [14], the step motor drives the rod, which is attached to the clamp ring with the membrane stick on it, through the pair of the gear and the gear rack (Fig.11). As the step motor rotating clockwise and anti-clockwise repetitively, the clamp ring moves upward and downward cyclically. This vertical displacement of the clamp ring results in the circular membrane stretched over a stationary indenter disk. The stretching of the membrane causes the cells' deformation, whose images can be obtained by the inverted microscope as the stationary indenter disk is transparent with a light source in it.

In addition, this device can be mounted on the regular microscope with certain promotion. For example, by adding a rectangular box to contain the upper part shown in the left illustration in figure 11, the whole device can be placed on the regular microscope.

Chapter 2. Project Strategy

Based on the introduction above, certain disadvantages of stretching devices, such as being costly, large dimension, and manufacturing complexity, still need to be overcome. This chapter is about the design strategy.

2.1 Objectives

In order to manufacture a membrane stretching device, several objectives of a new design are illustrated in this section. The target device needs to stretch the membrane at the deformation ratio from 0% to 50%. The reason to choose 50% as the upper limitation is that cells cannot survive when the ratio is larger than 50%. Furthermore, this device should be small enough to put on the microscope. In addition, the device should be friendly for the cells' survival during the working process. Lastly, this device should compensate for the disadvantages of current existing stretchers as mentioned above. Certainly, safety issues and adding a user interface should also be taken into the consideration. From the objective tree below, the goals of this device are clearly shown (Fig.12).

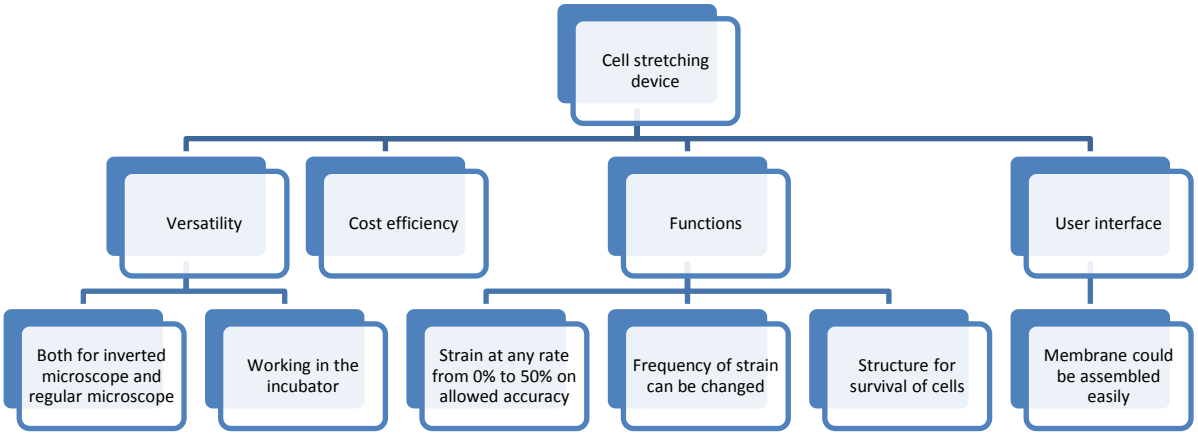

Figure 12: Objective tree of a stretching device

As shown above, the tree contains four main objectives. Those are the versatility, cost efficiency, multiple functions, and adding a user interface. This tree is helpful for choosing suitable stretching devices.

As mentioned previously, the stretching devices can be divided into three types through different power sources, such as electric motors, hydrostatic pressurization, and regulated vacuum pressure. According to working mechanisms, these devices can also be divided into three types such as uniaxial, equi-biaxial and radical. Based on the consideration of the uniformity of stretching processes, the radical stretching device is selected first. In the aspects of functions and adding the user interface, many types of devices can satisfy this situation if they are designed properly. Based on the consideration of the versatility, electric motors and regulated vacuum pressure should be selected as the power sources, due to their small size and simple structures. Considering the cost efficiency, stretchers with regulated vacuum

pressure should be removed from the alternative list, because this kind of devices is more expensive than any other type. Therefore, the outline of the new designed device, which will work radically by using electric motors, is clear.

2.2 Constrains

Constrains based on the working environment and conditions are the specifications that the final design should satisfy. This design will be mounted on the microscope to observe cells directly. Additionally, it can be put into the incubator. Taking the lab environment into the consideration, the inverted microscope is the working place for testing this device (Fig.13).

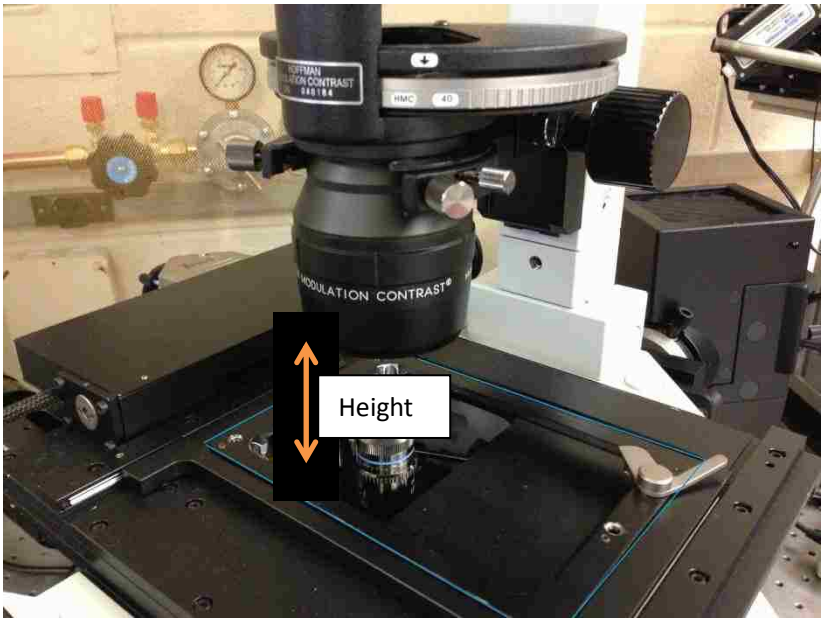

Figure 13: Microscope stage for the new device

The dimension of the stretcher is defined by the working environment. Since the inverted microscope has more environmental requirements than the incubator and the regular microscope, it should be taken into the consideration as the priority.

The blue line in figure 13 outlines the length and width of this device's base which will fit

into the stage to maintain the stability during the working process. The height of the device cannot exceed the orange arrow highlighted in the figure, otherwise it will intervene the working process of both the stretcher and the microscope.

Furthermore, to observe the cells cultured on the membrane, the device should have a hollowed structure. Besides, the area of this hollowed structure should be larger than the diameter of the objective lens. Through the measurement, the range of the whole device's dimension and the center hole are shown in table 1.

Table 1.Range of the dimension of cell stretching devices

Dimensions / Items	Length/mm	Width/mm	Height/mm
Whole device	154--160	106--110	0--90
Center hole	≥30 （Diameter/mm）		

From the data above, the dimension of the whole device is specified. According to the dimension of the center hole and the deformation ratio of the membrane, the vertical displacement of the working components can be calculated as shown below (Fig.14).

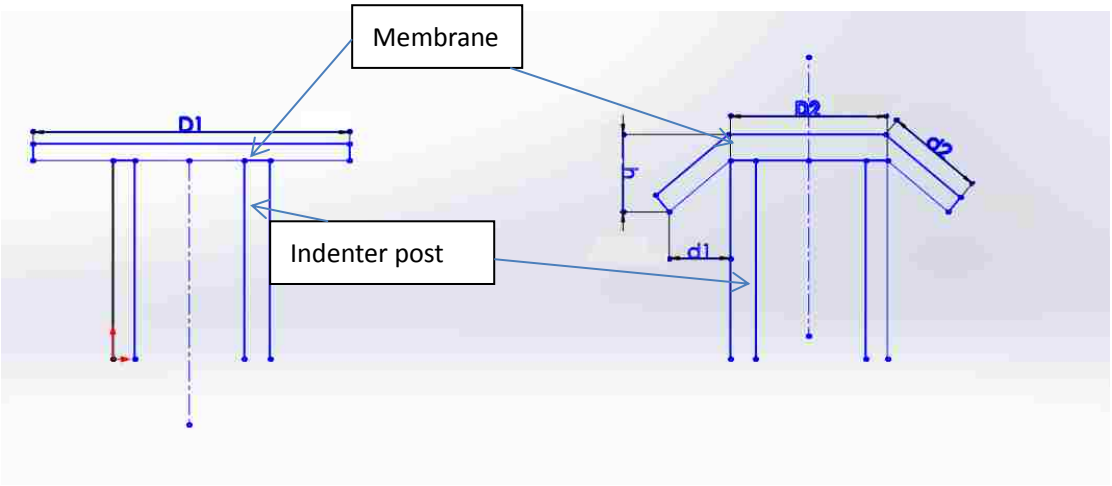

Figure 14: Schematic view of the membrane deformation

The left of the figure 14 shows the initial position of the membrane; the right one shows the deformed situation of the membrane. When the outer region of the membrane moves vertically, the stretching movement occurs. Based on the parameters in table 1 and the max range of the deformation ratio (50%), the maximum vertical displacement, h, can be calculated by using the following formulas:

$$D_1 - D_2 = 2d_1 \tag{1}$$

$$\frac{\pi(D_1+2d_2)^2}{4} \div \frac{\pi {D_1}^2}{4} = 1.5 \rightarrow \sqrt{1.5}D_1 - D_2 = 2d_2 \tag{2}$$

$$\sqrt{{d_2}^2 - {d_1}^2} = h \tag{3}$$

Where D_1 is the diameter of stretched region (outer region) of the membrane, D_2 is the diameter of the indenter post, and h is the max vertical displacement. From this data, constrains for this device can be finally specified.

Chapter 3. Design Alternatives

The idea of utilizing a vacuum pump rather than the stepper motor as the power source is considered at the beginning of the design. Besides the manufacturing complexity, it can satisfy the constrains and objectives mentioned above.

3.1 Alternative design using vacuum pump

This device can stretch the membrane radically by the vacuum pressure. The most important requirement for this vacuum machine is keeping the air tight. In order to meet this demand, each part should be bound together tightly as an integral. Considering the lab environment, this piece is manufactured by 3D printers which can accomplish complex structures, such as solid pieces with a hollowed structure in center. Therefore, the design of this device is separated into two parts, the vacuum base and the membrane.

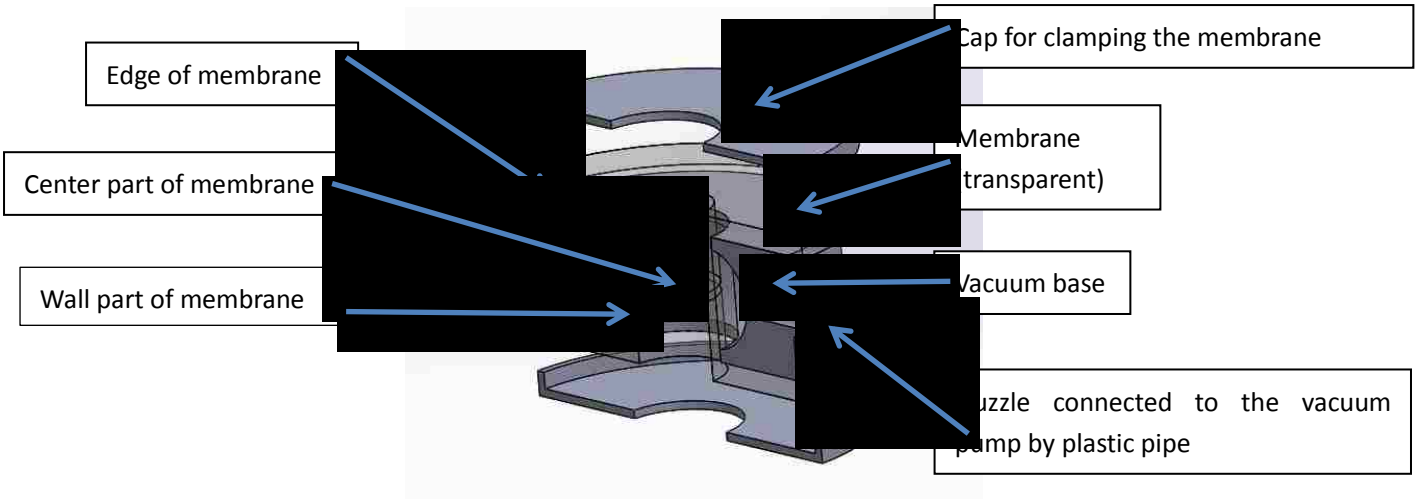

Figure 15.Section view of the vacuum stretching device

To stretch the membrane radically, the entire device is like a fat cylinder. The gap between caps and the vacuum base is smaller than the thickness of the membrane. Thus the upper and bottom caps (shown in Fig.15) can seize the membrane by the pressure, which can prevent

the air leakage. When the vacuum pressure is induced, the air in the hollow part of the base flows out of the four nuzzles around the circular surface. Until the vacuum pressure reached a certain level, the wall part of the membrane will deform outward which results in the expansion of the membrane's center part. The space of the hollow in the base can provide enough area for the deformation of the membrane at the ratio of 50%.

Since a circular hole goes through the entire device, cells should be cultured on a transparent membrane for a better observation on the microscope. The final design of this device is shown below (Fig.16).

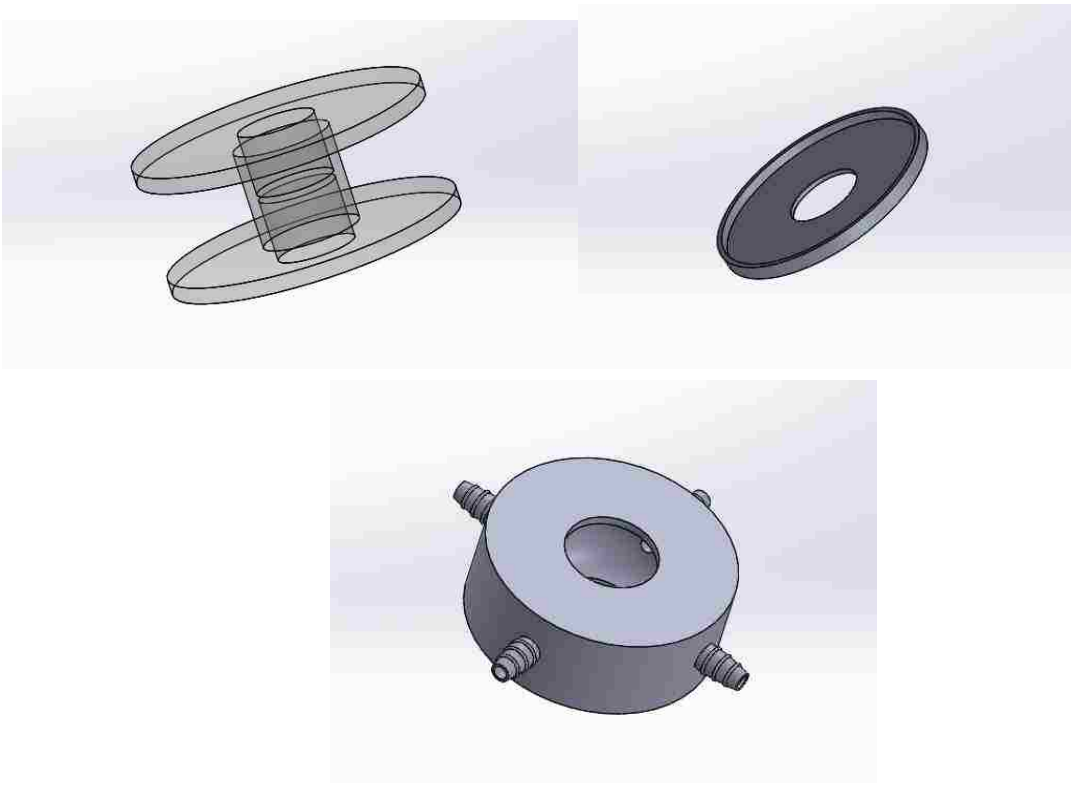

Figure 16: Components of the vacuum device: Membrane (upper left); Clamp cup (upper right); Vacuum base (lower middle)

However the vacuum base made by 3D printers has been cracked for during several printing processes. Besides, the manufactory of the membrane is another problem. The membrane can be made of the mixed silicon-based liquid. Therefore, a mold for the

membrane must be fabricated first. Since the mold made of the metal is too expensive, the decision is to use a silicon rubber as the mold material (Fig. 17).

Figure 17: Membrane mold made by the silicon rubber

The fabricating process of this mold is successful. However it is difficult to separate the membrane and the mold completely. In addition, several issues still need to be solved, such as the way to control the vacuum pump. According to these problems, this plan has been changed with a new idea of utilizing the electric motor as the power source, which can be easily accomplished by 3D printers.

3.2 One step motor design

In this design, the step motor (Fig.18-1) is used to drive two pairs of gears (Fig.18-2) and gear racks with a pair of compacted circular plate on which a circular membrane is mounted (Fig.18-4). The membrane anchor plate (Fig.18-5) fixes the membrane on the surface of the gear rack part (Fig.18-3) by four pairs of bolts and nuts. The gear assembled on the motor's rod can rotate clockwise and anti-clockwise, which makes the gear rack part move upward and downward repetitively.

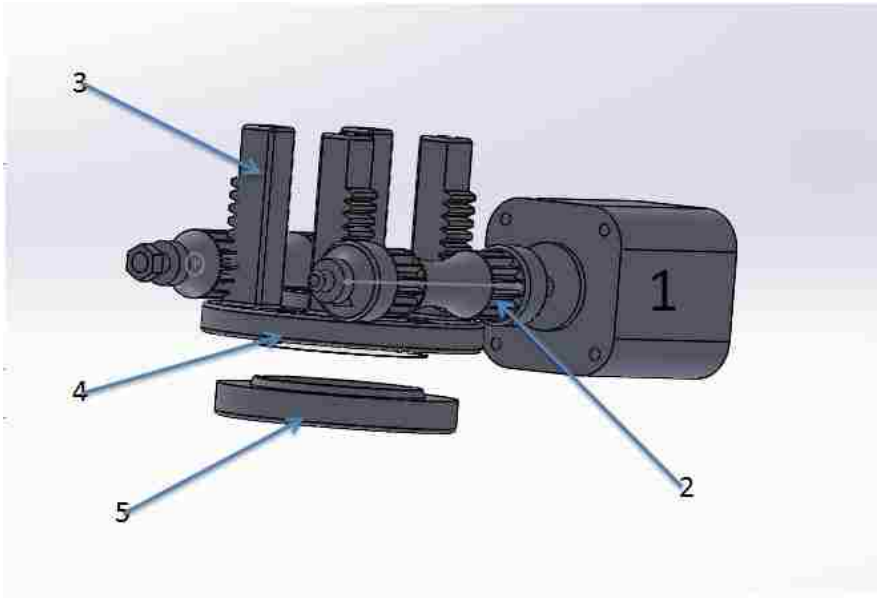

Figure 18: Part view of one motor design: 1.step motor; 2.gear; 3.gear racks part; 4.transparent membrane; 5.Membrane anchor plate

The base (Fig.19 A-1) mounted with the step motor has indenter posts (Fig.19 A-2) in the center. The posts are manufactured by the 3D printer. During the working process, the motor case and base are kept in a stationary status. As the gear rack part (Fig.19 D-2) moves upward and downward, the edge of the membrane will move accordingly while the center of the membrane (Fig.19 D-3) is still kept in the same vertical position by the indenter posts (Fig.19 D-1). Therefore the deformation of the cells cultured on the membrane can be observed during this process.

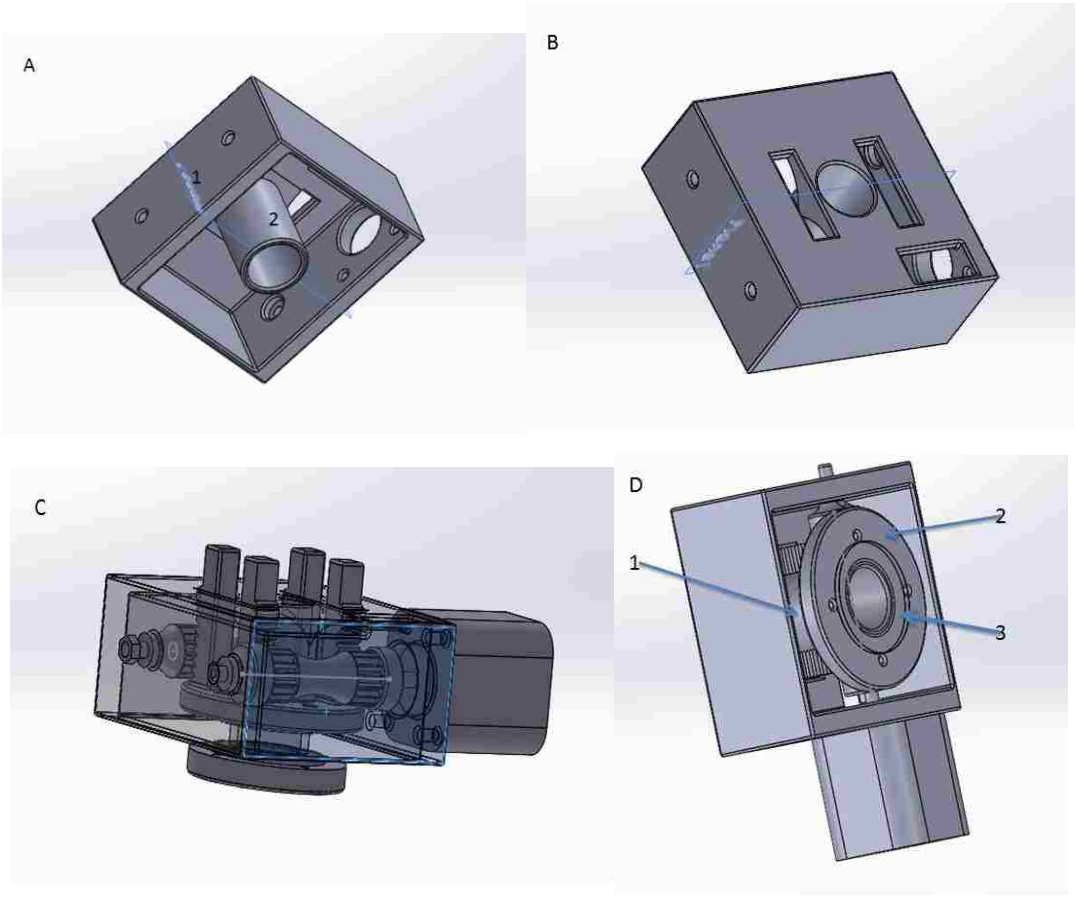

Figure 19: Schematic view of one motor device: A-1.base for the whole device; A-2.indenter post; D-1.indenter post; D-2.gear racks part; D-3.membrane

In above figures, the four gear racks are set around the indenter post, which can allow the light of the microscope to go through the membrane. Two pairs of gears and gear racks can keep the stability of the whole system. The thickness of each plate is at least 5mm. Since the plane with thickness less than 3 millimeter cannot endure the force for a long time.

The most impressive thing of this design is the gear rack part. In Figure 19-B and C, two rectangular holes on the top of the base can allow the feet of gear racks to penetrate through. The size of these holes is just a little bit bigger than the area that the feet of the gear racks occupy. Such a design can assist in specifying the location of the gear rack part. In the middle of the plate, a wall structure (Fig.20-1) will hold the media for cells.

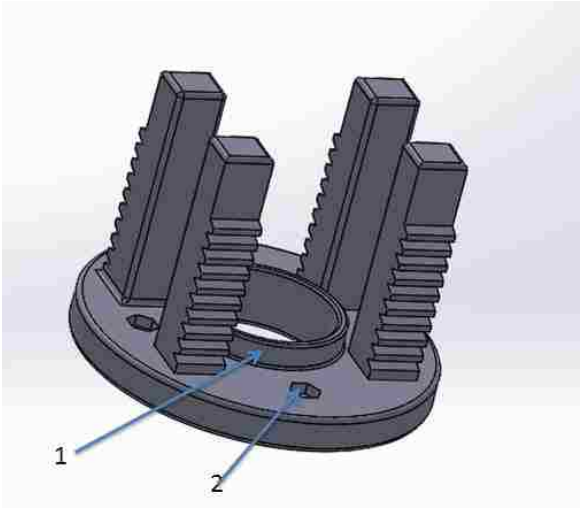

Figure 20: Gear rack part: 1.Wall structure; 2.Four hex holes on the plate

The function of the four hex holes (Fig.20-2) is to anchor the nuts. This structure increases the thickness of the plate, because another thickness of the nut should be taken into the consideration. At the beginning of this design, this wall structure does not exist because the cells can be seeded on the other side of the membrane, which is more convenient to observe by inverted microscope. However if there are nano particles planted on the membrane together with cells., this wall structure is necessary to prevent the falling of nano particles.

3.3. Two motors design

The difference between the two motors design and the one motor design is not significant. The former one only has one more motor symmetrically along the center line of the whole device. Although this change is not obvious from appearance, it can affect the stability of the device during the working process.

When the electric motor is under the free condition (without power on) the rod can rotate if a torque is induced. As the motor has been initialized by the electric current, the rod will be seized by the motor itself, which contributes to the stability during the working process. In

one motor design, the gear rack part will tilt even if one of the gears is seized by the motor since the other one is still under the free condition (Fig.21).

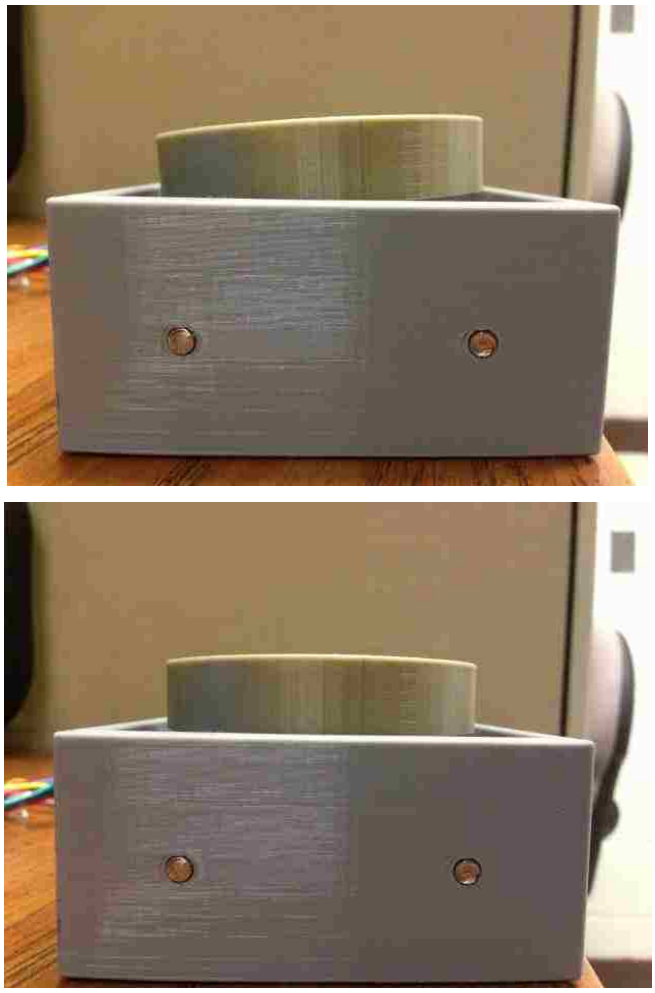

Figure 21: Comparison the stability of the device with one motor (upper) and two motors (lower)

Based on the comparison of the figure above, the advantage of two motors design is obvious. The following figure is the modeling of the two motors design (Fig.22).

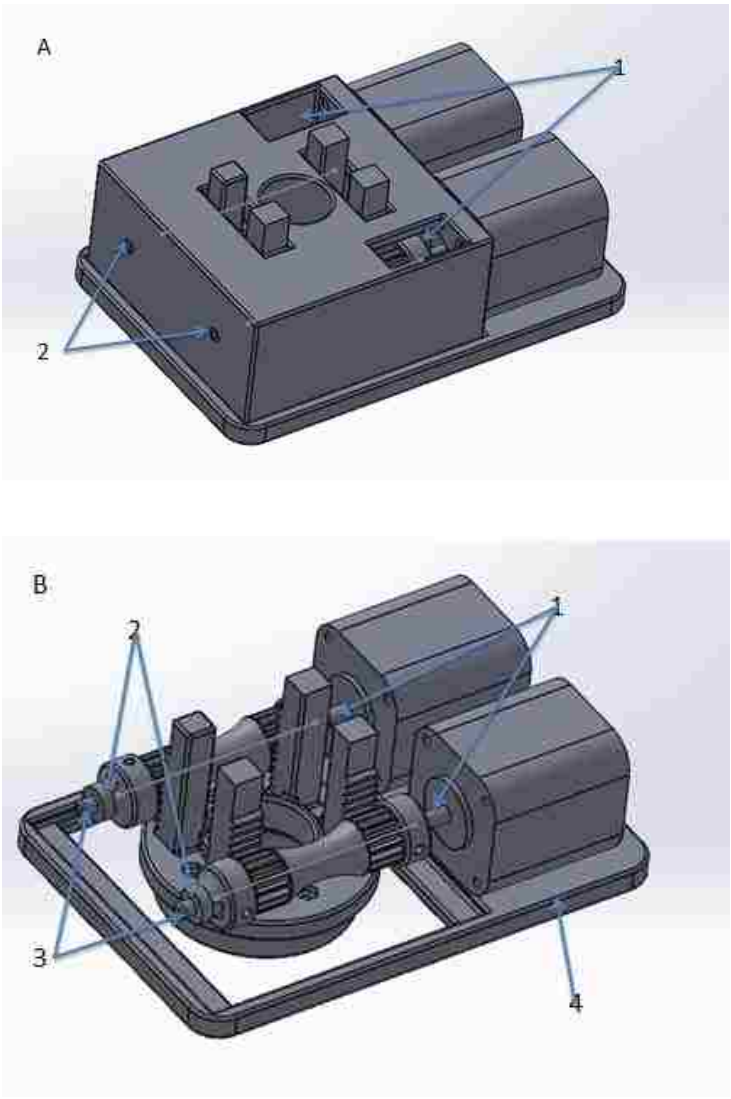

Figure 22: CAD for the two motors design in two different view: A-1.Two rectangular holes; A-2.Two pin holes; B-1.Motor rod; B-2.Bearings; B-3.Pins; B-4.Bottom plate

The whole device is placed on a bottom plate (Fig.22 B-4) whose dimension fits the length and width of a microscope stage. The rectangular holes (Fig.22 A-1) are used to assembling the motors on the base. The pins (Fig.22 B-3) anchored on the gears can be mounted in the pin holes (Fig.22 A-2). Along with pins, there are two bearings whose function is to make the pins rotating smoothly and steadily.

Chapter 4. Parameters of the design

The two motors design is the final decision. Several data and parameters should be obtained through calculations and experimentations, which are mainly described in this chapter.

4.1. The chosen of electric motors

The entire design is influenced by the size of electric motors, which are divided into three types: step motors, servomotors and linear motors. The linear motor, which is also called linear actuator, should be removed from the alternative list. This kind of motors can translate the torque and rotational motion into the linear force and movement. However, this motor must be set vertically for the radical stretch, which results in the similar design shown in figure 8 that cannot be put on the microscope.

Servomotors can convert the electric current into the torque which is contrary to a linear actuator. By utilizing the negative feedback which is used as the investigation of the difference between the actual position and the desired position, the servomechanism controls the motor rotational position [10] whose accuracy depends on the error signal.

Step motors generate the toque by the magnet. Different designs of step motors have different accuracy, which is depend on the number of steps of a full rotation. It is easier to maintain step motors than servomotors. The price of them is lower than servo motors too. They do not lose steps or require encoders if operated within their design limits[11]. In addition, the servo motors are better served when the RPM is above 2000 or higher which is not suitable for membrane stretchers.

Therefore, step motors are the final decision. There are many types of step motors to be chosen. NEMA 17 step motors can provide enough torque and rotational resolution, which induce enough force on the membrane as well as provide an accurate control.

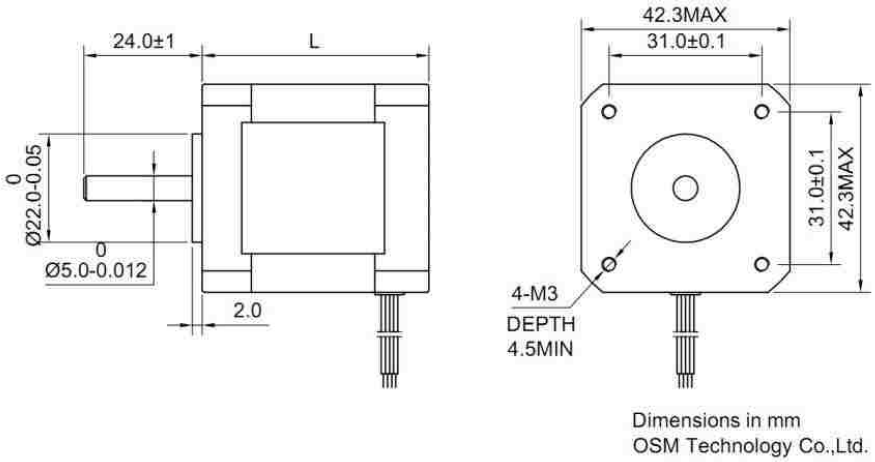

Figure 23: Detailed dimension of Nema 17 step motor

From the side view of this motor (right in Fig.23), both the width and height of this motor are the same. If two motors are set aligned as shown in Fig.22, the minimum width of the bottom plate is 84.6mm.

Four screw holes on the motor are used to assemble the motor on the base. Utilizing three or two of these holes can make the motor fixed steadily on the base. Therefore, three holes on the anchor plane of the base are used to assemble the motors.

4.2. Calculation of parameters

According to constrains of this device, the range of basic parameters (Table.1) and the formulas for the calculating data is determined. First of all, the size of the device must satisfy the dimension of the microscope stage. In table.1, the length, width and height of the microscope stage are 154mm – 160mm, 106mm – 110mm and 0mm – 90mm respectively.

The length and width of the bottom plate are 159mm and 106mm (Fig.24 A). In Fig.22 A and Fig.19, the height of the gear racks part is bigger than the base. Thereby the height of the gear rack is the criterion to measure the total height of this device.

However the gear rack part moves upward and downward during the working process, the distance of the vertical displacement must be taken into the consideration as well. In this case, the total height of this device is its vertical displacement adding the height of the gear rack part (Fig.24 B).

According to formulas (1), (2) and (3), the diameter of the indenter post can be calculated. In addition, the diameter of the center hole of the anchor plate (Fig.24 D), which is larger than the indenter post, should be confirmed. Thus, this hollowed structure can provide enough area for stretching. Otherwise the indenter post and the membrane will be stuck in this hole since the gear rack part moves towards the indenter post (Fig.24 E).

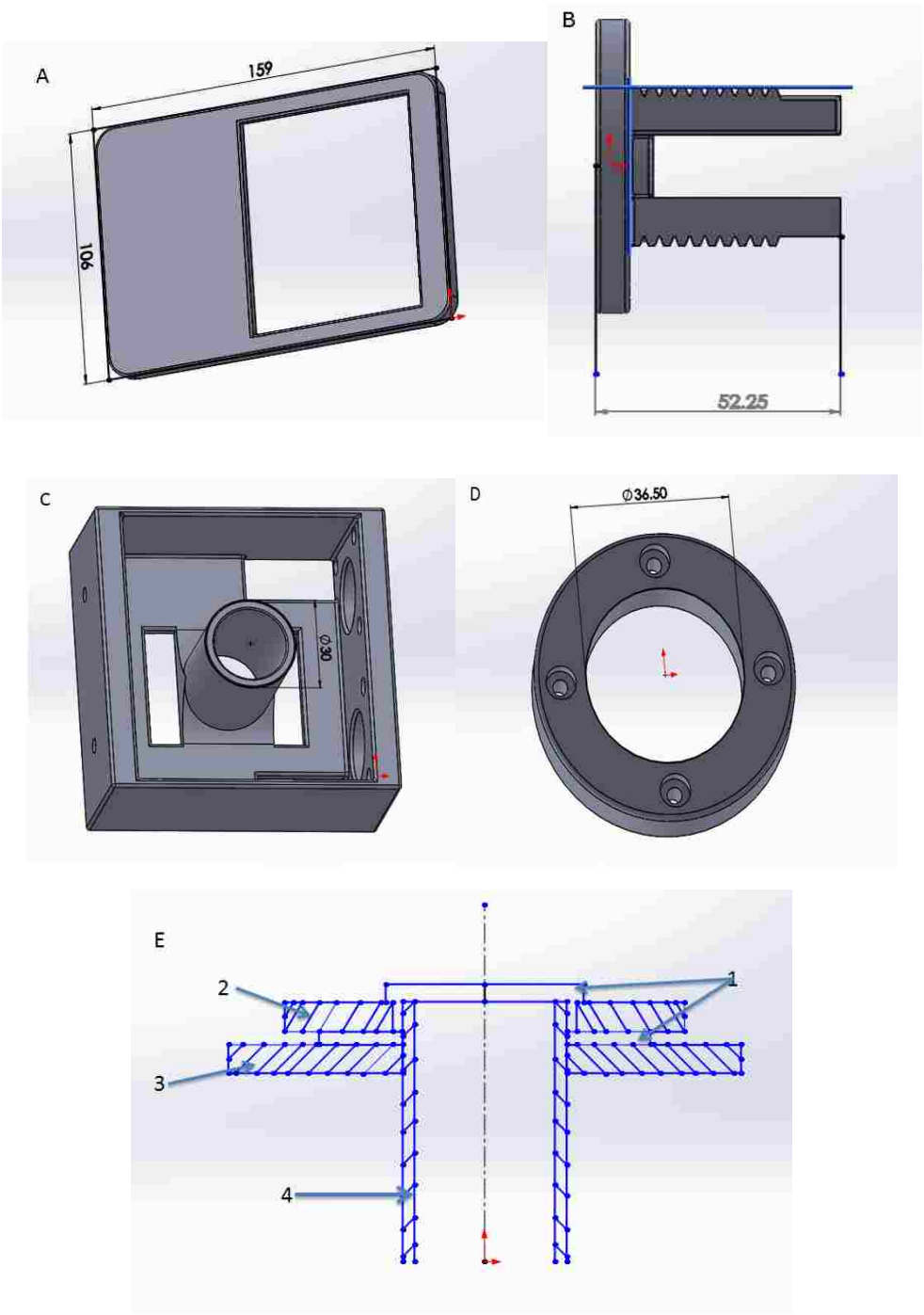

Figure 24: Dimensions of the different part: A. Length and width of the bottom plate; B. Height of the gear rack part; C. Diameter of the indenter post; D. Diameter of the center hole of the anchor plate; E. schematic view of the membrane stuck by the anchor plate: 1. Membrane; 2. Anchor plate; 3. Gear rack part; 4. Indenter post

The diameter of the center hole on the membrane anchor plate has been set as 36.5mm (Fig.24 D), which is enough for membrane stretching. From the figure above, the diameter of the indenter post is 30mm (Fig.24 C), which meets the range shown in table.1. Consequently,

the parameter of D_1 and D_2 (formulas.1, 2 and 3) can be calculated. Similarly, d_1 and d_2 are 7.35mm and 3.25mm from which the max distance (6.6 millimeter) of the vertical displacement is obtained. Before adding this distance to the total height of this device, the dimensions of gears and gear racks should be measured (Fig. 25 C).

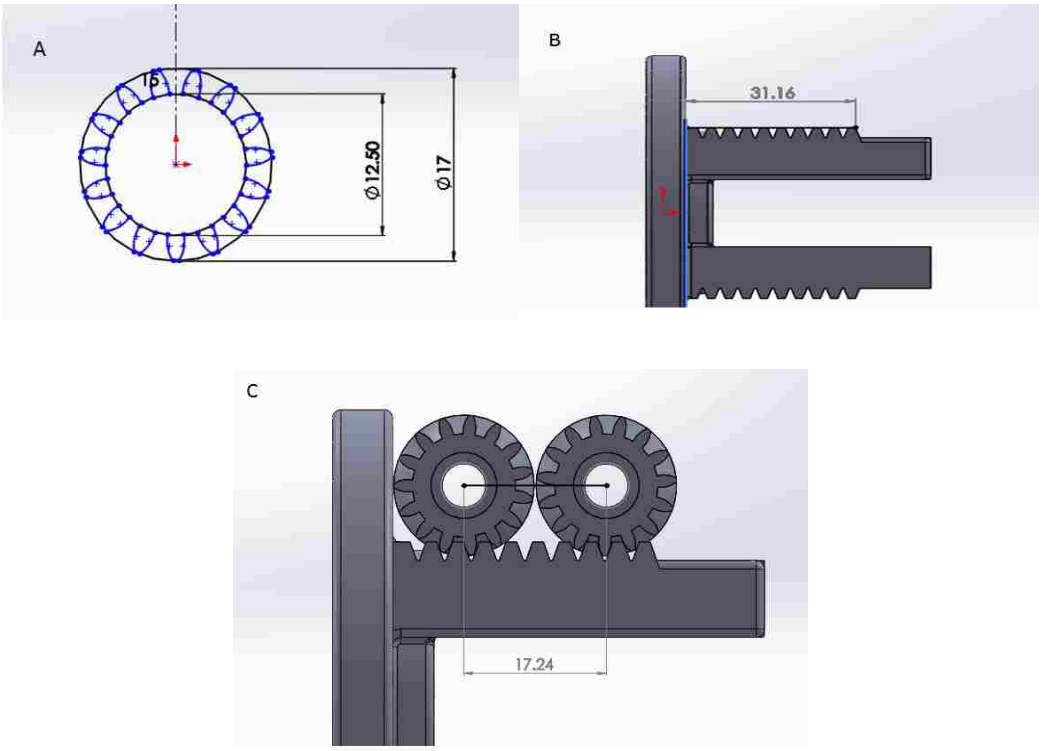

Figure 25: Several specific dimensions of the gear and gear rack: A. Diameter of the gear; B. Length of the gear rack; C. Moving range of the gear and gear rack

The diameter of the gear is 17mm (Fig.25 A), and the length of the gear rack is 31.16mm (Fig.25 B). According to this, the working range of the gear and gear rack group can be calculated as 17.24mm, which is much larger than 6.6mm. Contrarily the dimension of the biggest hole of the anchor plate can be attained by utilizing the formulas above. This working range (17.24mm) can be regarded as the max distance of the vertical displacement. Therefore the calculated diameter of the biggest hole of the anchor plate is 64.08mm.

4.3. Other parameters

As discussed above, two step motors will be set aligned along the wide side on the bottom plate. This needs the width of the base to be at least 84.6mm. By considering the width of the bottom plate (106mm), the outer region for the holding base is set at least 3mm on each side. Therefore, the width range of the base is from 84.6mm to 100mm.

To confirm the length of the base, the length of step motors should be known firstly. However, this data is different because of the various designs of Nema 17 motors. Table.2 shows the data of Nema 17 step motors, the longest and shortest motors are 48mm and 34mm respectively.

Table 2.Specification of Nema 17 motors

Manufacturer	Holding torque	Rated voltage	Motor length
3D Acessories Hub	43 N/cm		42 mm
Kysan	54.0 N/cm	4.2 V	48 mm
Kysan	54.0 N/cm	4.2 V	48 mm
Kysan	88 N/cm	2.6 V	48 mm
LDO Motors	50 N/cm	2.8 V	47 mm
Longs Motor	40.0 N/cm	2.6 V	40 mm
Mercury Motor	23.0 N/cm	12 V	34 mm
RobotDigg	28.0 N/cm	4.8 V	34 mm
RobotDigg	40.0 N/cm	2.0 V	40 mm
RobotDigg	65.0 N/cm	4.05 V	60 mm
SOYO	31.1 N/cm	4.0 V	40 mm
SOYO	55.0 N/cm	2.8 V	47 mm

Manufacturer	Holding torque	Rated voltage	Motor length
SOYO	43.1 N/cm	2.8 V	48 mm
SOYO	43.1 N/cm	2.8 V	48 mm
Thingibox	35.3 N/cm	2.8 V	36 mm
Thingibox	35.3 N/cm	2.8 V	36 mm
Wantai	47.0 N/cm	3.1 V	48 mm
Wantai	49.0 N/cm	3.6 V	48 mm

The longest version is the final decision. After decreasing the length of motors, the left part of the bottom plate is for the base. Furthermore, by adding the dimension of the outer region on each side of the bottom plate (at least 3mm), the length range of the base should be less than 105mm.

The lower limitation of the base will be confirmed by the design of the gear racks. In the center of the gear racks, the diameter of a circular wall is 36mm (Fig.26 A). Four feet of the gear racks are set around this wall to prevent the intervening of the vertical movement. The area where the four feet occupied forms a rectangular shape whose length of the diagonal line is 65.6mm (Fig.26 A).

The membrane is clamped between the gear rack part and the anchor plate by four pairs of M3 screw bolts and nuts.

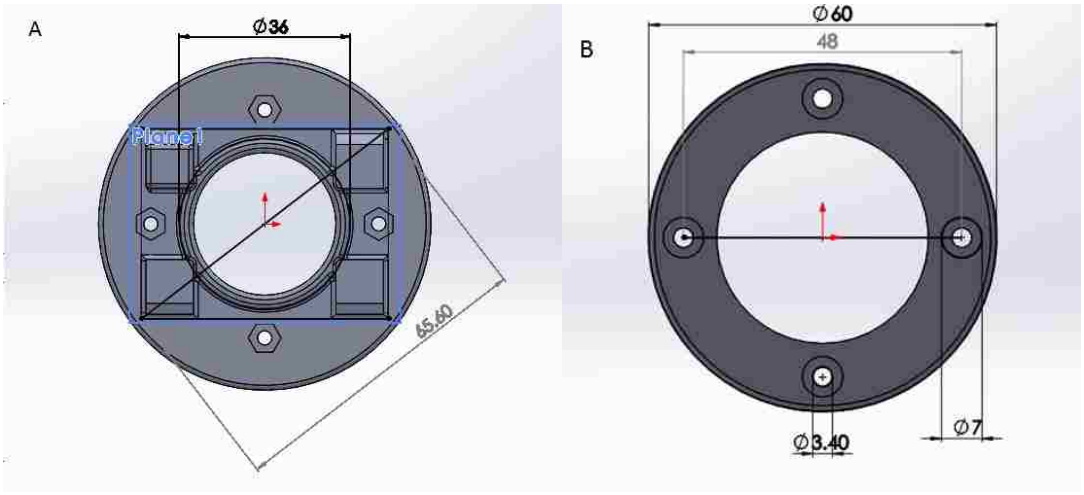

Figure 26: Dimension of the gear rack part (A) and anchor plate (B)

Four circular holes (Fig.26 B) for the bolt head are on the anchor plate. The head diameter of M3 bolt is 5.5mm. The diameter of these holes is set as 7mm, due to the tolerence of 3D printer. Similarly, the hex holes in design (Fig.26 A) are a little bit larger than the nuts. After adding 7mm, the distance of two holes on the diagonal line is 56mm (Fig.26 B). Consequently, the diameter of the outer circle of the anchor plate is 60mm. After adding the length of the outer region and the diameter of the bottom plate, the diameter of the gear rack part is 70mm. In addition, 10mm width of the gear rack is less than the width of the gear. Such a design can provide enough space to adjust the relative position between the gear and gear rack.

The lower limitation of the base length is 80mm based on the consideration of the base thickness. Thereby the final range of the base, whose length is from 80mm to 105mm and the width is from 84.6mm to 100mm, has been determined. The base is a hollowed center cuboid with the indenter post in the middle, which is manufactured by a 3D printer as an integral (Fig.27).

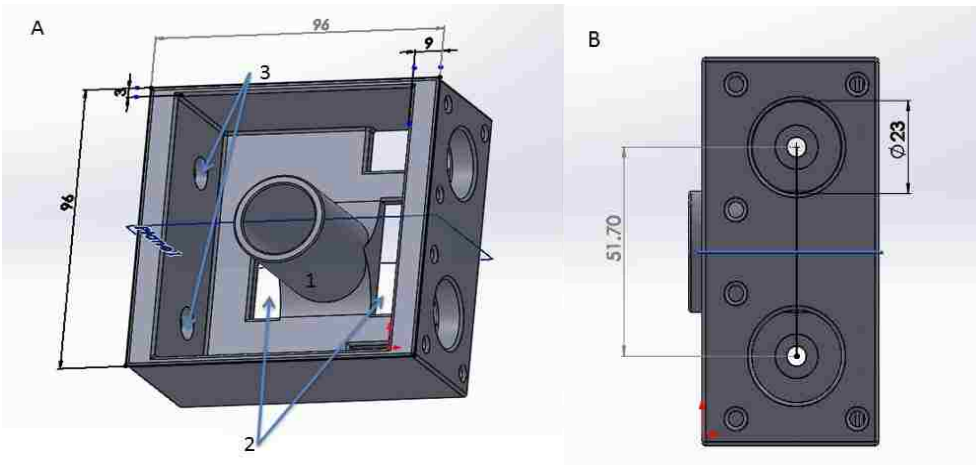

Figure 27: Data of the base: A-1.Indenter post; A-2.Rectangular holes facilitating the gear rack part assembly; A-3.Circular holes for the bearing; B: Center distance of two motors

The thickness of the plane mounted with motors and bearings (Fig.27 A-3) is 9mm, since the plate with thickness less than 4mm will be cracked under the screw force. The thickness of other two sides is 3mm resulting from no force endured on these two planes. Both the length and width of the base are 96mm, which give enough area for setting two motors aligned with a 51.7mm center distance (Fig.27 B). There are two larger round holes (Fig.27 B) to make the gears put through. The height of the base must be less than the height of the gear rack part that is 52.25mm. In this design, the height of the base is 45.15mm.

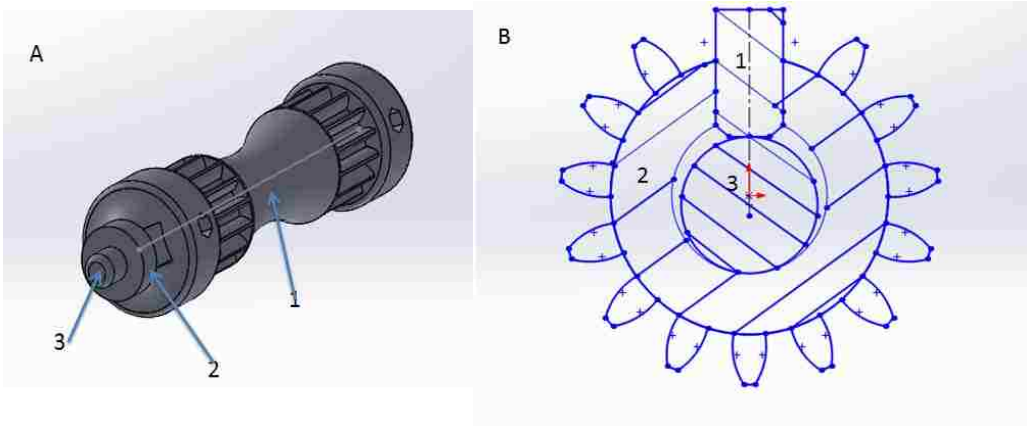

Figure 28: Schematic view after assembling the gear and pin together: A-1.Gear; A-2.Bearing; A-3.Pin; B-1.Grub screw; B-2.Gear; B-3.Pin

The gear and pin are connected by the grub screw and nut as shown above (Fig.28 B). The

grub screw induces the force on the pin that makes the center of the pin and gear staying at the different location. Thus the hole of the pin on the base must endure unbalanced forces when the gear starts rotating. To solve this problem, a bearing is stuck in the base tightly to hold the pin that can maintain the stability of the working process (Fig.28 A). The size of the selected bearing is 5x11x4 with a 5mm hole to match the pin. 11mm is the diameter of the outer circle and 4mm is the thickness of the bearings.

The gears are also made by 3D printers. This measurement gives the number and the height of the teeth for reference to assist the design of the gear rack. Before printing the pair of the gear and gear rack, experimentations should be made to testify if this pair can work well. Here is the sample of a pair of the gear and gear rack (Fig.29).

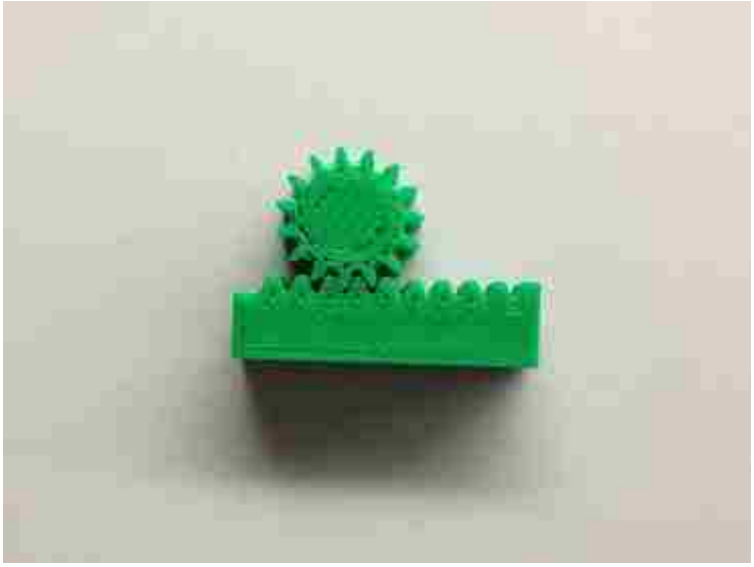

Figure 29: Sample of the partial assembly of the gear and gear rack

This figure shows the gear can match well with the gear rack to maintain the device stability. From above three sections (4.1 to 4.3), the majority of parameters have been confirmed for the further design and revision.

4.4. Substrate design

The membrane are required to be in a circular shape for the radical stretching, transparent for the observation, soft for the easy deformation, elastic for returning to the initial condition, and cost efficient. Membranes bought from manufacturers are too expensive. For instance, the price of StageFlexer® membranes sold by the Flexcell Corporation [12] is around 50 dollars for only 6 membranes. In addition, not being recyclable is a huge cost on experiments. Therefore, many investigators find other ways to fabricate the membrane.

PDMS is the most commonly used material due to its transparency and elasticity. Many experiments have certificated that the cells can be cultured on it successfully. The manufacturing process is not difficult: 1.Mixing the curing agent and the PDMS base sufficiently for a couple of minutes at a certain ratio; 2.Pouring the mixture into the mold; 3.Putting the mold into the vacuum pump for several minutes to remove the air bulb mixed in the liquid; 4.After removing all the bulbs, moving the mixture into the oven for hours at a certain temperature to cure.

It is reported that these four steps influence a lot on properties of PDMS. For instance, changing the ratio of the curing agent and the PDMS base, the degree of mixing and temperature setting of the oven can affect the ductility, strength and stretchability of the final product. The culture dish is a proper mold of membrane, because of its circular shape, transparency and smooth surface.

To test the durability, the PDMS membrane is clamped between two plates. After several hours of stretching test, this membrane deformed too much without force induced on it. This means the error of deformation will become larger and larger by using the PDMS membrane

during the working process. To solve this problem, a new membrane material, which is called Solaris®, is selected. Solaris® is a kind of rubber like material with low viscosity and high transparency. Here is the table of parameters' comparison between the PDMS and Solaris®.

Table 3.Parameters' comparison between PDMS and Solaris®

Material of membrane	Tensile modulus (MPa)	Elongation at break (%)	Shrinkage (%)
184-PDMS	1.8	160	1.1
h-PDMS	8.2	7	1.6
s-PDMS	0.6	70	3.1
hv-PDMS	3.4	54	0.6
Solaris®	25	290	＜0.1

According to this table, the elongation at break (the most important property) of Solaris® is much higher than the PDMS. This property is partially affected by the tensile modulus. The lower the shrinkage is, the more accurate the volume of liquid mixture can be measured. The manufacturing process of Solaris® is simpler than the PDMS, that is: 1.Mixing the curing agent and the silicon base at ratio 1:1 thoroughly; 2.Pouring the mixture into the mold; 3.Moving the mold to the vacuum pump to remove the air bulb; 4.Putting the mold on a flat surface at room temperature (73 ℉/23 ℃) for 24 hours until the mixture cured. It is necessary to notice that this material cannot be cured when the temperature is less than 65 ℉/18 ℃. The useful temperature range of Solaris® is from -149 ℉ to 400 ℉ (-100 ℃ to 205 ° C), which means this membrane can be sterilized by the steam around 150 ° C. But it is better to use the

UV light to sterilize to prevent the deformation.

Cells can be cultured on the membrane made by Solaris®, which has been tested successfully after several hours of experiments. However the region for culturing cells should be specified, because cells will not survive when they are touched by the indenter post during the stretching process. The data collected by the experiments will invalid once some of the cells die when contacting the indenter post. In this case a circular groove is fabricated on the membrane. Thus cells can be cultured within the boundary marked by this groove (Fig.30-2).

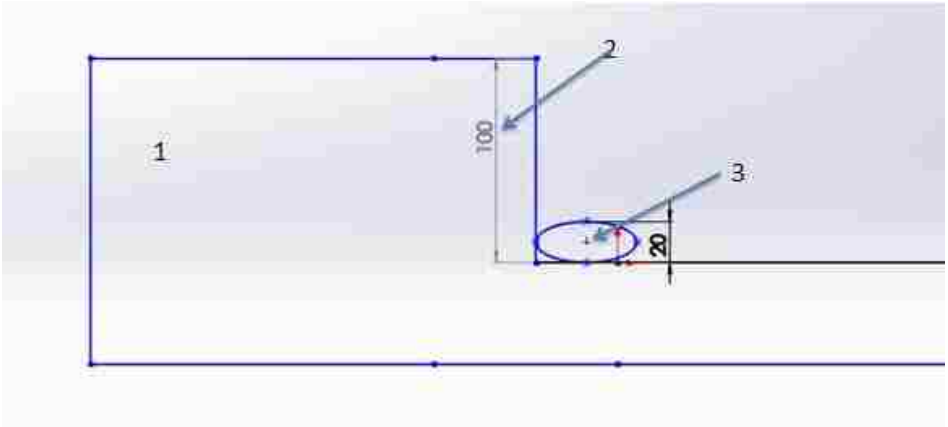

Figure 30: Schematic view of new design membrane: 1.Membrane; 2.Circular groove on membrane; 3.One cell

It is reported that the average height of cells is around 20 micrometer (Fig30-3). For security considerations, the depth of the circular groove is 100 micrometer, which is really small compared to the thickness of the membrane (1mm). Therefore, the influence of this groove on properties of the membrane can be neglected. In addition, the dimension of this groove must be confirmed under the max deformation ratio (50%) conditions, which can be calculated by the following formulas:

$$\frac{\pi {d_3}^2}{4} \times 1.5 = \frac{\pi {d_4}^2}{4} \quad (4)$$

$$d_3 = d_4 \div \sqrt{1.5} \quad (5)$$

Where d_3 is the diameter of the groove, d_4 is the diameter of the inner circle of the indenter post. The diameter of the inner circle of the indenter post is 24mm, and the diameter of the groove is 19.59mm. The cells cultured into this groove will just reach the indenter post at 50% deformation rate by using this parameter. Additionally, an outer region of the membrane should be taken into the consideration. Therefore, the final dimension of the groove diameter is 16mm.

However, a new issue comes out that is how to make this groove on the membrane. It is too difficult to manufacture this groove precisely by hand or any other machines directly. The only choice is fabricating this groove and the membrane together. In this situation, a mold must be designed for this membrane (Fig.31).

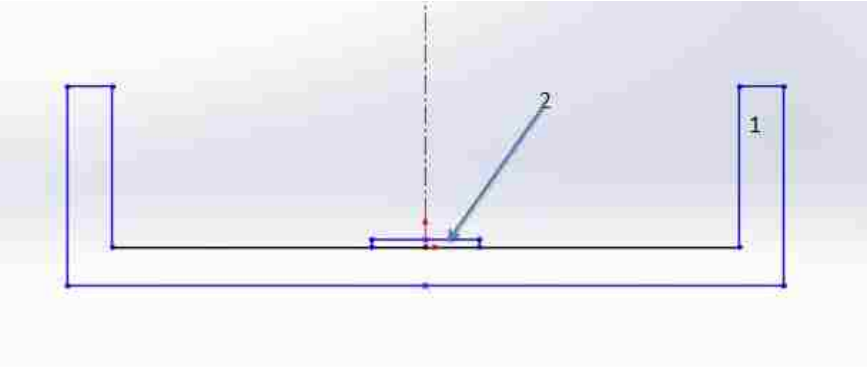

Figure 31: Schematic view of the mold for the new membrane: 1.Mold; 2.100 micrometer high plate

Utilizing adhesive tapes, whose range of the thickness is from 60 to 120 micrometer, can solve this problem (Fig 32). After cutting the tape into a specific shape according to designed dimensions, it will adhere to the center of the mold. The new membrane is accomplished once the mixture has been poured on it.

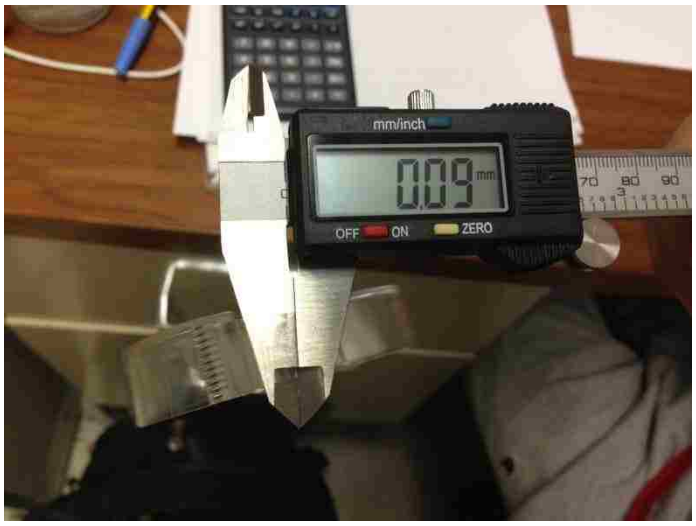

Figure 32: Thickness of the plastic tape

4.5. Motor control

The step motor is controlled by the software – Pronterface, which is the interface to control a 3D printer that usually uses Nema 17 step motors to drive machines. The step motor is controlled by a computer through a PCB board which gets power from a 24V supply to run step motors directly. The board is connected to a computer by USB cable respectively (Fig.33).

Figure 33: Open SL 1.0 Control Board

On a Nema 17 step motor, four cables are coated with different color aligned in a certain

sequence. The motor is connected to the board by these cables. However, there are two motors in this design. In this case, the two motors must rotate in a contrary direction which is solved by connecting these four cables in a reverse order. Therefore the board can control these two motors simultaneously by outputting the same signal.

The software, Pronterface, uses G-code to control the movement of step motors. After loading the G-code file (written below) into the software, clicking the “Print” button on it the software can control the motors’ movement.

G code

G91

G1 Z-0.17 F22

G1 Z0.17 F22

G1 Z-0.17 F22

G1 Z0.17 F22

G1 Z-0.17 F22

G1 Z0.17 F22

G1 Z-0.17 F22

G1 Z0.17 F22

G1 Z-0.17 F22

G1 Z0.17 F22

G1 Z-0.17 F22

G1 Z0.17 F22

G1 Z-0.17 F22

G1 Z0.17 F22

G1 Z-0.17 F22

G1 Z0.17 F22

G1 Z-0.17 F22

G1 Z0.17 F22

G1 Z-0.17 F22

This code is just the repeat of two lines, which controls the motors to rotate clockwise and anti-clockwise cyclically at a certain angel and frequency. After repeating enough amounts of these two lines, this device can work for enough time as required. The parameters behind the Z and F in this code represent the displacement on Z direction and frequency respectively. Since this software is designed for 3D printers initially, the unit setting on this software cannot fit this stretching device. Through adjusting these parameters step by step, the relationship between the vertical displacement and the angel of motors' rotation, which is linear, can be determined. For instance, when the deformation ratio of the membrane is 20%, the vertical displacement is 3.79 mm and the parameter of Z is 0.17. Consequently, the relationship between the parameter of Z and the vertical displacement can be concluded. Similarly, the deformation ratio of the device can be changed by the modification based on this relationship (Fig.34).

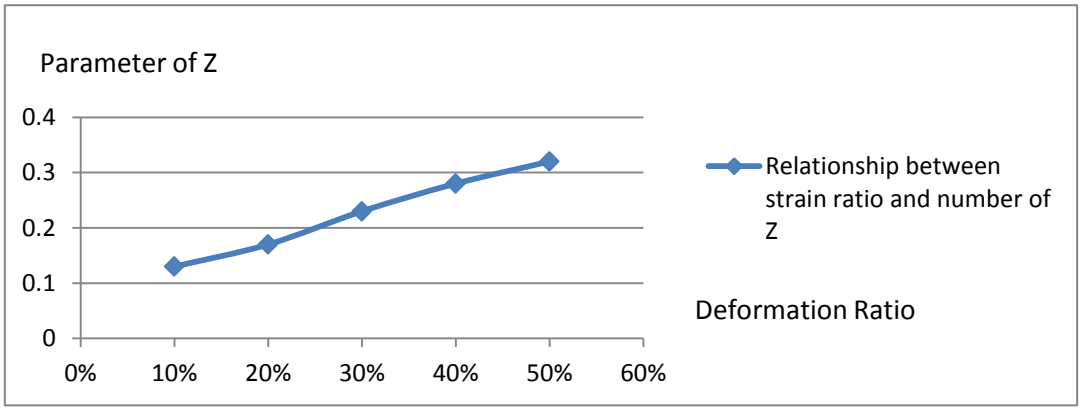

Figure 34: Relationship between the deformation ratio and parameter of Z

In summary, this chapter discussed about the reason of selecting step motors, measurements and calculations of various parameters which are vital for the design, manufactory, and control. This is just a preliminary result of the entire design. Only after the promotion through experiments, the final design of this membrane stretcher can be obtained.

Chapter 5. Test and Final design

5.1. Assembly and Test of stability and leakage

All the components of this device are manufactured by 3D printers, which extrude melted plastic through a nozzle to build pieces layer by layer. There are several advantages of this kind of machines. For instance, the piece with complex structure can be manufactured as an integral. This can only be accomplished by the manufacturing of several individual pieces in other methods. However this machine has several limitations, especially the accuracy and surface finishing. It can meet the requirements of the working precision of this stretching device. The following figure is a partially assembled model of this device (Fig.35).

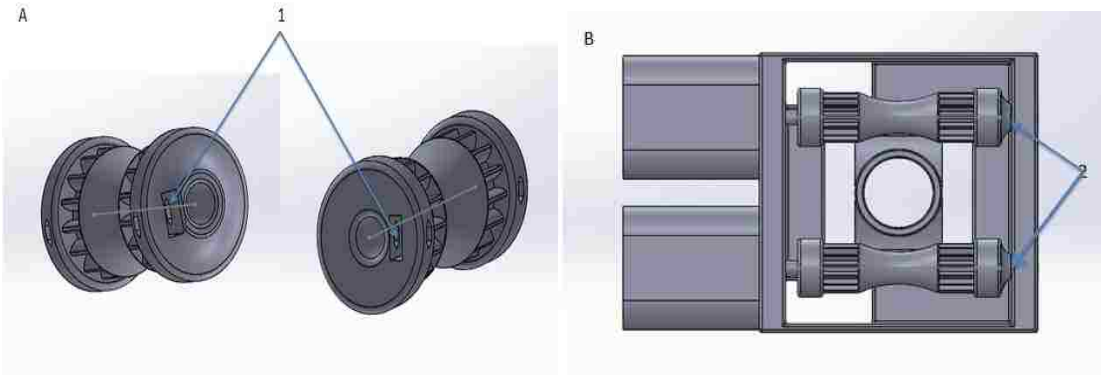

Figure 35: Partial assembly process of the stretching device: A-1.Holes for holding the grub screw nuts; B-2.Relative position between gears and base

As shown in the figure above, the grub screw nuts and bearings are anchored in the holes of the gear (Fig.35 A-1) and the base respectively (Fig.35 B-2). Secondly, gears, motors and pins are combined by grub screws as an integral whose relative position is determined by the dimension of the base (Fig.35 B). Thirdly, two motors are mounted on the base by six M3 screw bolts. Finally, the gear rack part, membrane and anchor plate are assembled by four pairs of bolts and nuts. But a leakage test of this part should be made before assembling it

into the base. In the case of no forces being induced on the membrane, there is no leakage happening after a several hours' test.

The whole device can work stably during the two hours of stretching test. The vertical movement of the gear rack part is smooth. However, the liquid leaked from the fission between the plate and the membrane. The reason of leakage is not the insufficient force applied on the membrane and plates, but the existence of little grains on the plate (Fig.36).

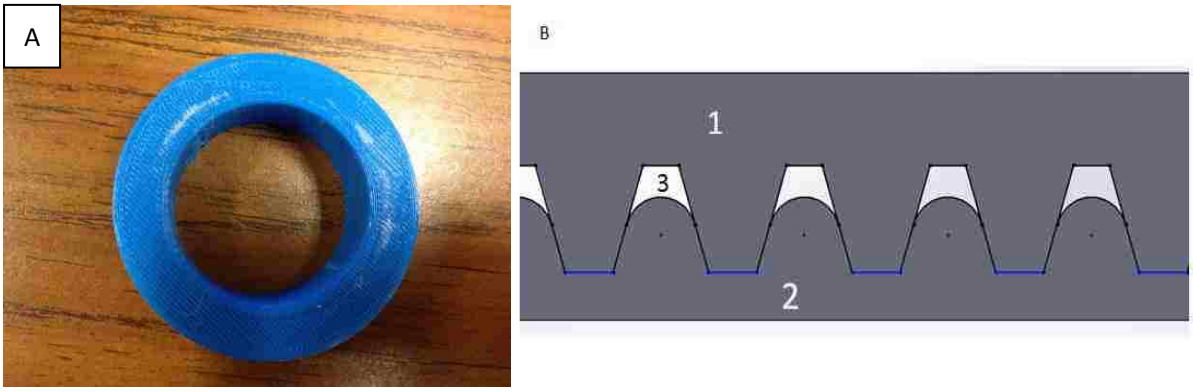

Figure 36: Flaws of the piece made by the extrusion printer: A. Little grains on the plate made by 3D printers; B. Microcosmic view of the contact between the membrane and plate: 1.Plate with the little grains; 2.Membrane after seized by the force; 3.Fisson between the plate and membrane

Due to the existence of these little grains (Fig.36 A), the membrane and plates cannot be seized tightly no matter how significant forces supplied by bolts. The fission (Fig.36 B) between them allows the media flowing through it, especially during the working process which enlarges this fission.

This issue is solved by a new design of an anchor plate and a gear rack part. The groove and wall structures on the gear rack plate and the anchor plate is the key (Fig.37).

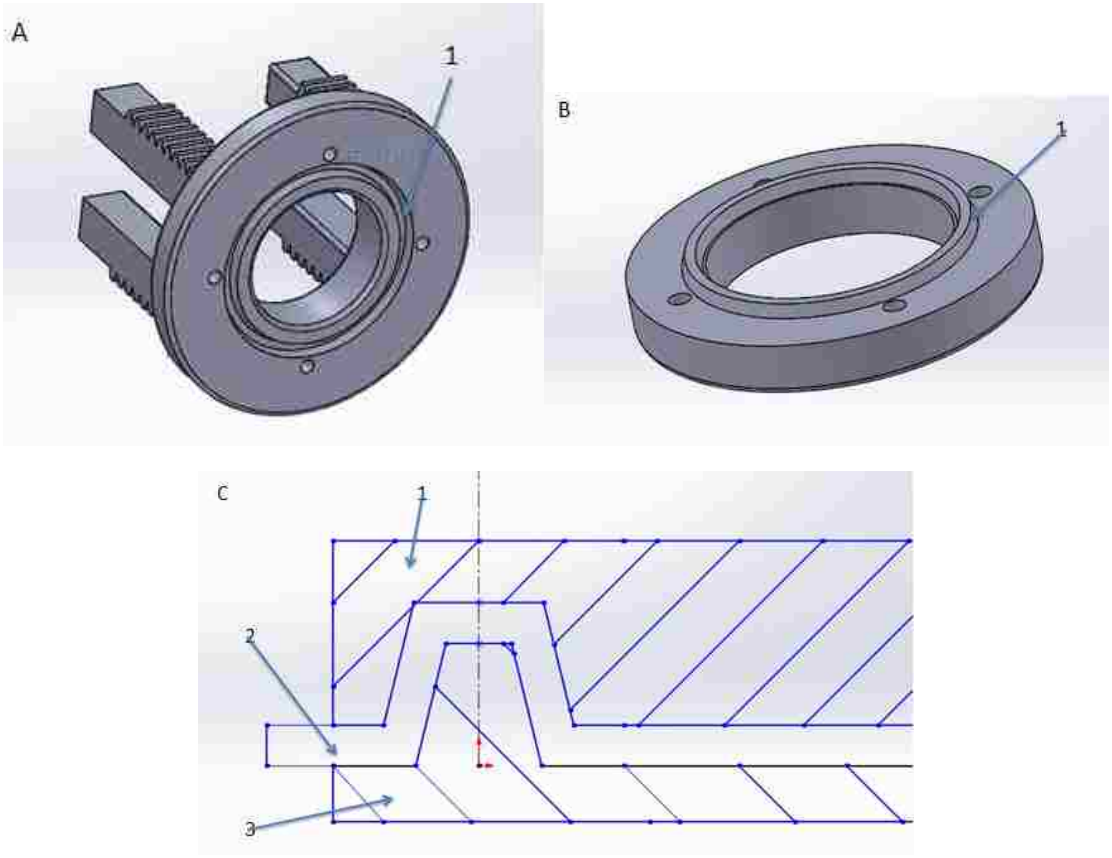

Figure 37: New design to solve leakage: A-1.Groove on gear rack plate; B-1.Wall on anchor plate; C-1.gear rack plate; C-2.Membrane; C-3.Anchor plate

In this design, the edge of the membrane is clamped between the groove structure on the gear rack plate (Fig.37 A) and the wall structure on the anchor plate (Fig.37 B), which prevents the media leaking from the fission among the membrane and plates. However, the membrane made by Solaris® is cut by shear force after assembling these three pieces together. Only the PDMS membrane can sustain this force at a certain thickness. Therefore, another new design is put forward that induces pressure among the membrane and plates without bolts and nuts.

5.2. Final design

In former design, four holes are drilled on the membrane to ensure the penetration of screw

bolts. These holes damage the membrane partially. It will cause the membrane tearing especially during the working process. To avoid this problem, the final design uses threads to make the working component tight (Fig.38).

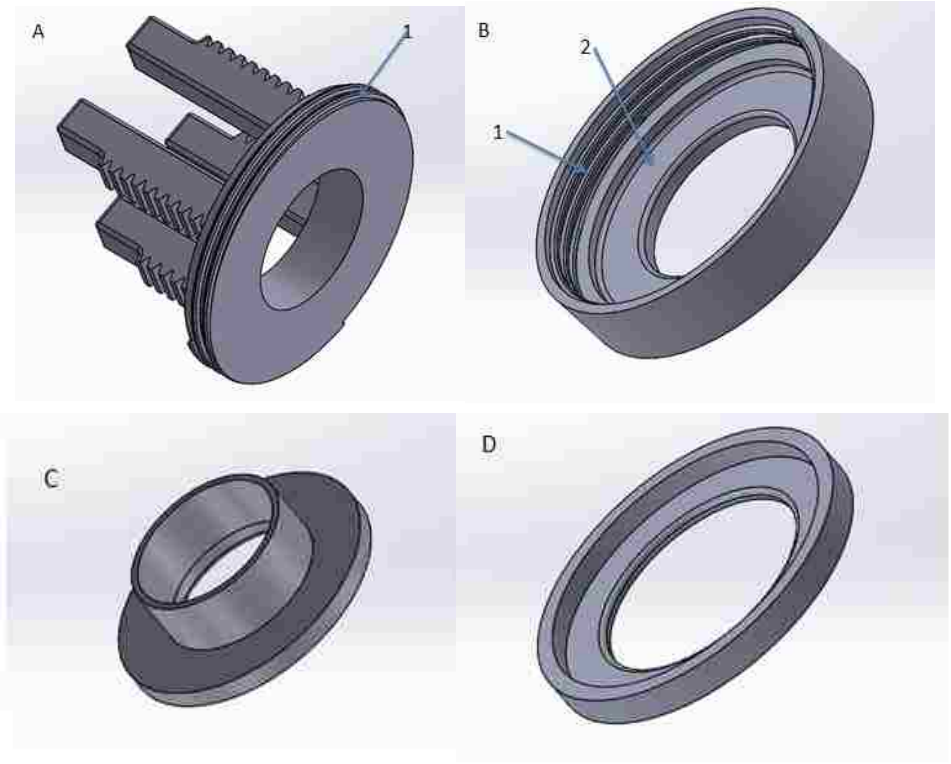

Figure 38: New working part of the final design: A-1.External thread on the gear rack part; B-1.Internal thread on the anchor cup; B-2.Locating the circular groove; C.Culture plate; D.Membrane holding cup

The pressure seizing the membrane is generated from the threads on the gear rack part (Fig.38 A) and the anchor cup (Fig.38 B). However, the membrane cannot be put on the gear rack plate directly due to the relative rotation, which can result in the scratch of the membrane. This issue is solved by the design of the culture plate (Fig.38 C) and the membrane cup (Fig.38 D).

These two parts are manufactured by a 3D printers.. As a result, the leakage problem is solved due to the removal of the fission between the membrane cup and the membrane.

The inner circle diameter of the membrane cup should be a little bit larger than the culture

plate’s diameter. Therefore, these three parts can be combined as an integrity, which will be put into the circular groove on the anchor part (Fig.38 B-2) to assist in locating the membrane at the center position. Thus, the membtane’s scratch problem is solved (Fig.39).

Figure 39: Assembly of all parts for the woking component: 1.Membrane

5.3. Parameters of new parts and test of final design

Before manufacturing these new parts, several parameters should be measured and calculated. Actually, only one dimension should be measured, which is the outer circle diameter of the anchor cup whose 76mm length meets the inner length of the base (78mm). However, the inner circle diameter (D_1 in formulas (1), (2) and (3)) of the membrane cup has changed, which influences the deformation ratio. This new dimension is 40mm (larger than former design), which meets the upper limitaion of D_1 (64.08mm). Therefore, to keep the same deformation ratio, the parameter of Z in G-code should be adjusted accordingly.

However in this final design, the diameter of the culture plate’s hole is too small to be put inversly. This part can only be used on an inversed microscope. To make this device working

on a regular microscope, another new culture plate is designed. The only adjustment is the hole's diameter (36.5mm) of the culture plate and the diameter of the wall structure. Therefore, different culture plates can use the same membrane cup. In this way, this stretching device can be put on both inverted microscopes and regular microscopes (Fig.40).

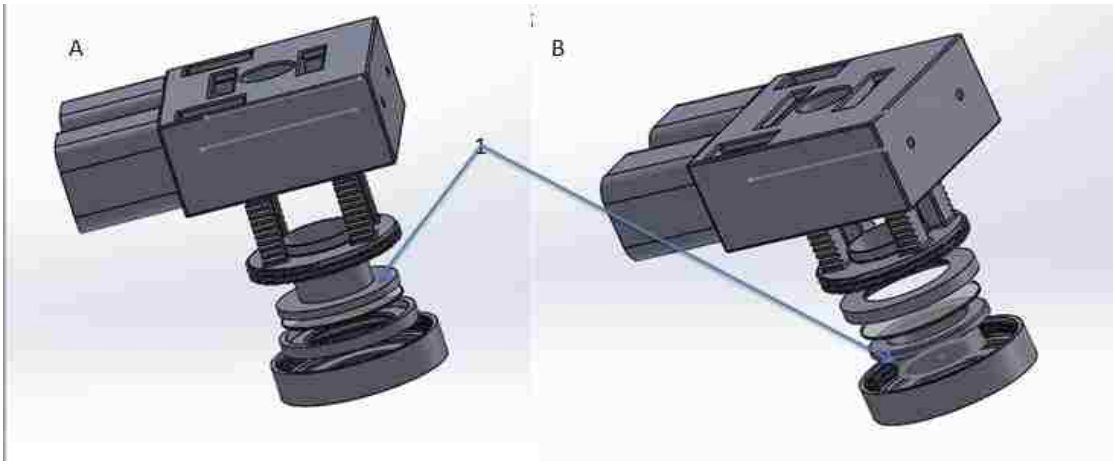

Figure 40: (A) Device used for the inverted microscope; (B) Device used for the regualr microscope; 1: The difference between these two mode

After manufactring all these pieces, the most important thing is to test the leakage, stability and deformation ratio of this final design. No leakage happened after more than two hours' testing. During this process, the gear and gear rack can work soomthly and stably. Figures below show the results of leakage and stability test.

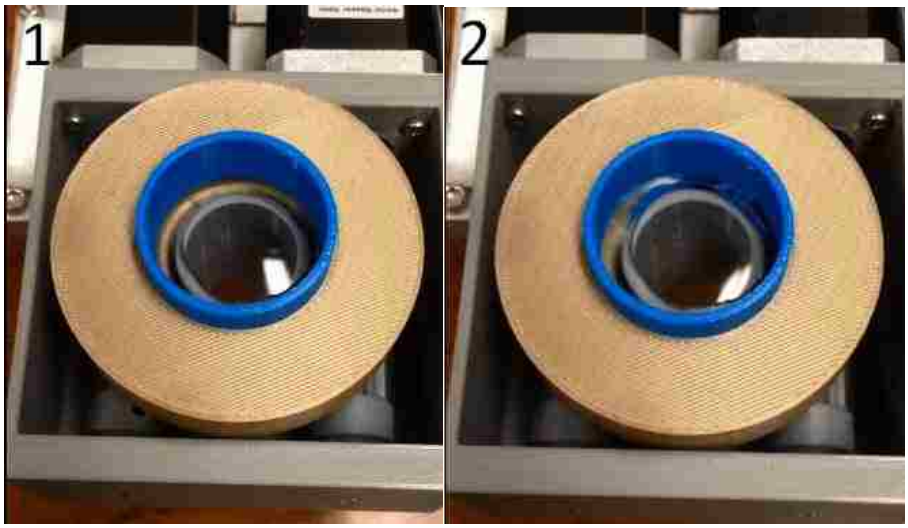

Figure 41: Test of the leakage and stability 1.Membrane at the initial position; 2.Membrane stretched

Deformation ratio of this design can be adjusted according to demands. Here is the data (Table.4) of the relationship among the deformation ratio, vertical displacement and the parameter of Z.

Table 4: Data of stretching ratio

Stretching ratio	Vertical displacement/mm	Parameter of Z (G-code)
10%	3.273	0.15
20%	4.768	0.21
30%	5.992	0.27
40%	7.076	0.32
50%	8.072	0.36

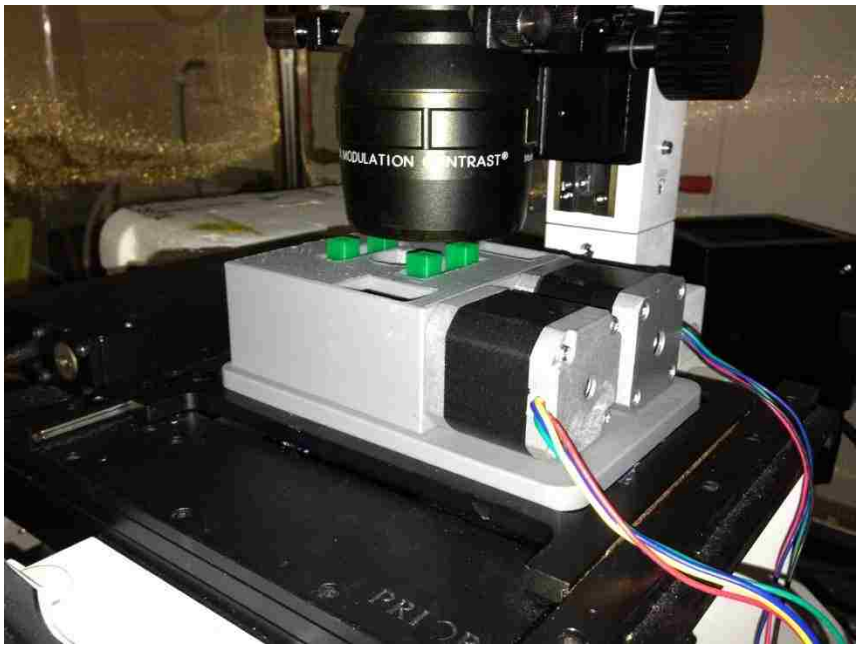

Figure 42: Device working on the inverted microscope

The above figure shows how the device is mounted on the microscope (Fig.42). By comparision with other existing devices introduced previously, this final design has

advantages like: 1.This design can stretch the cells radically to induce multiple forces on the cells after making comparisions with many uniaxial and equi-biaxial devices; 2.This design can be put on the microscope to observe directly due to its hollowed center structure while most of radical stretching devices cannot; 3.This design is easy to move because of its small size aomparing with many other devices; 4.The replacement of membranes is simpler while majority of other devices using complex method of applying bolts and nuts to fix the membrane. Bolts and nuts not only damages the membrane but also are hard to assemble.

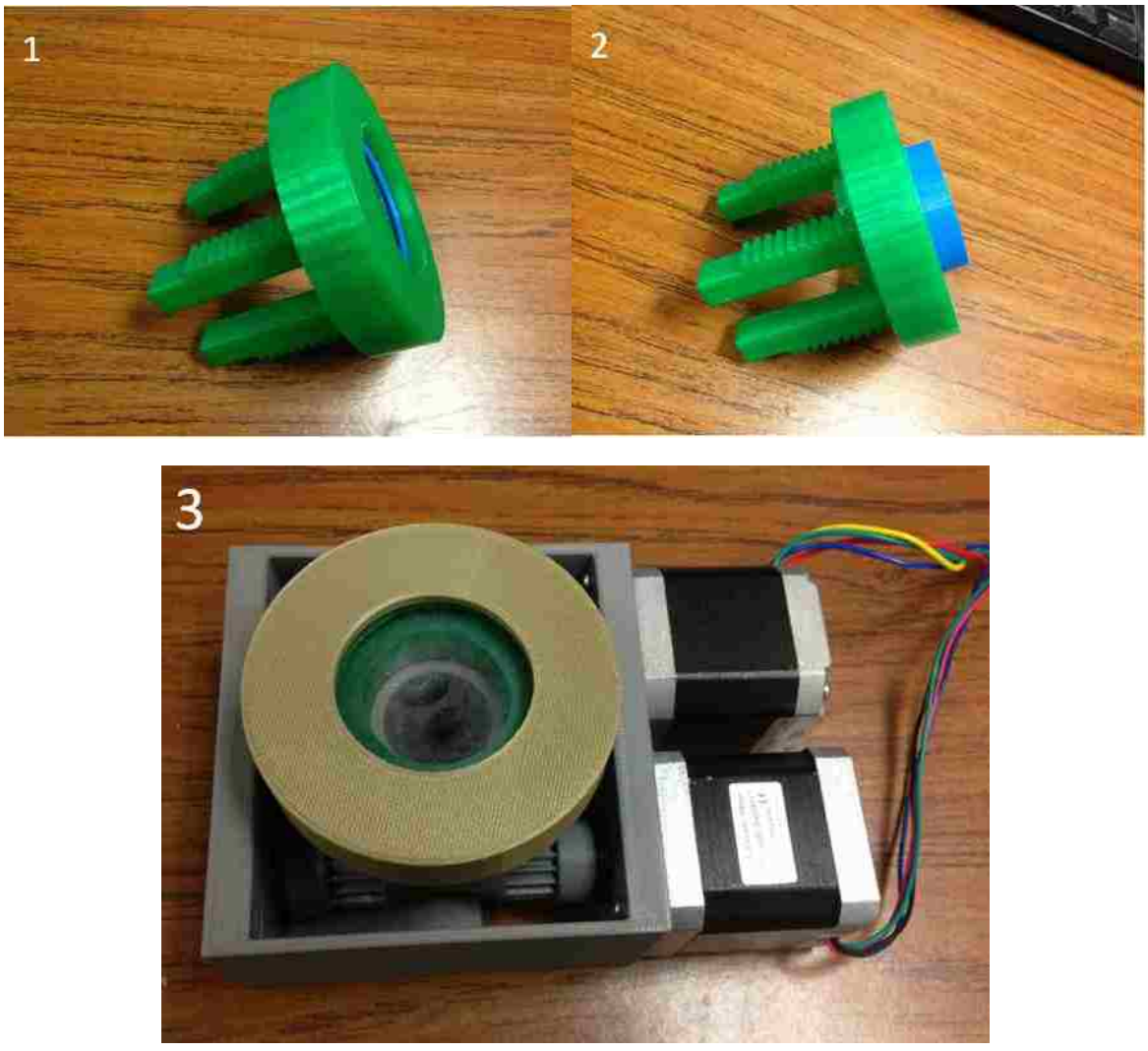

Figure 43: The image of the final design: 1.Assembly of working part for the inverted microscope; 2.Assembly of working part for the regular microscope; 3.The entire membrane stretching device

The above figure is the image of the final design that satisfies all the objectives listed in the section 2.1 (objectives). They are versatility, cost efficiency, multi-functions and being user friendly. First of all, it can work both on the microscope and in the incubator. Secondly, the manufacturing cost of this device is less than 300 dollars. Thirdly, this device can adjust the deformation ratio and frequency at certain accuracy. Furthermore the structure of the culture plate guarantees the survival of cells. In addition the assembly and dismantle of the membrane is more convenient.

5.4. Future improvement of this device

This device is expected to have more kinds of mechanical stimulations rather than only one type of stretching currently. With further design revision, this design can stretch two types of cells simultaneously after applying a new step motor which has two rods on it (Fig.44).

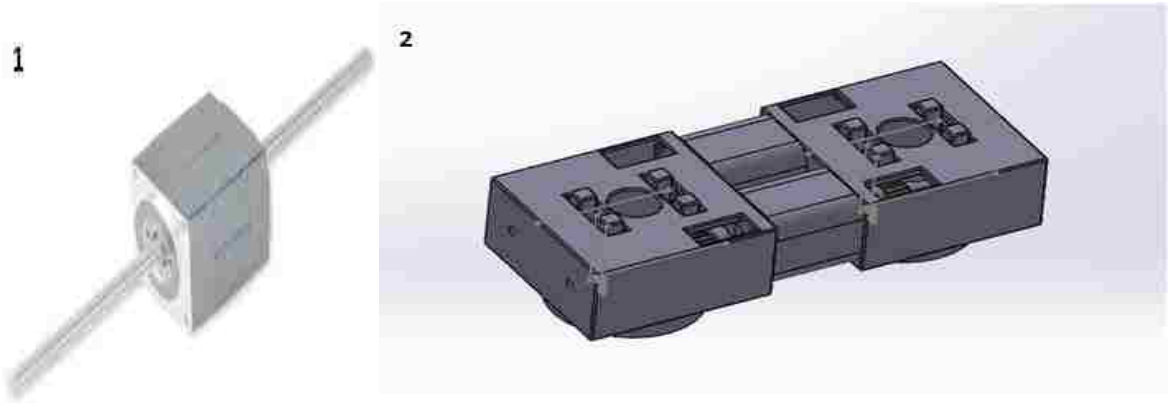

Figure 44: 1.Motor with two rods; 2.Future device with two rods motor

Besides, the entire device is made of plastic, which cannot be sterilized by hot steam whose temperature is around 150 ℃ (the melting point of plastic is 220 ℃). The gear rack part will broke during the working process, because the working component becomes fragile after two hours' sterilization. The only way of sterilization is using the UV light whose sterilizing

effect is worse than the hot steam. In future design, the entire device will be made of the metal. Thereby the device will endure the high temperature. However, the structure of the base and the gear racks part is too complicated, which cannot be made of metal as an integral. The only method is assembling these two parts by several pieces whose structure is simple enough to manufacture.

Reference

1. Wang J, Thampatty B. An introductory review of cell mechanobiology. Biomechanics and Modeling in Mechanobiology 2006; 5(1):1-16.

2. Throm Quinlan AM, Sierad LN, Capulli AK, Firstenberg LE, Billiar KL. Combining dynamic stretch and tunable stiffness to probe cell mechanobiology *in vitro*. PLoS ONE (8):e23272.

3. Hsu H, Lee C, Kaunas R. A dynamic stochastic model of frequency-dependent stress fiber alignment induced by cyclic stretch. PLoS ONE (3):e4853.

4. Goodman CA, Mayhew DL, Hornberger TA. Recent progress toward understanding the molecular mechanisms that regulate skeletal muscle mass. Cell Signal 2011 12; 23(12):1896-906.

5. Pietramaggiori G, Liu P, Scherer SS, Kaipainen A, Prsa MJ, Mayer H, Newalder J, Alperovich M, Mentzer SJ, Konerding MA, Huang S, Ingber DE, Orgill DP. Tensile forces stimulate vascular remodeling and epidermal cell proliferation in living skin. Ann Surg 2007; 246(5):896,902 10.1097/SLA.0b013e3180caa47f.

6. Chin MS, Lancerotto L, Helm DL, Dastouri P, Prsa MJ, Ottensmeyer M, Akaishi S, Orgill DP, and Ogawa R. Analysis of neuropeptides in stretched skin. Plast Reconstr Surg 2009; 124(1):102,113 10.1097/PRS.0b013e3181a81542.

7. Wang J, Li B. Mechanics rules cell biology. Sports Medicine, Arthroscopy, Rehabilitation, Therapy & Technology 2010; 2(1):16.

8. McCullen SD, Haslauer CM, Loboa EG. Musculoskeletal mechanobiology: Interpretation by external force and engineered substratum. J Biomech 2010 1/5; 43(1):119-127.

9. Thomas D B. Techniques for mechanical stimulation of cells in vitro: A review. J Biomech 2000 1; 33(1):3-14.

10. Lipt åk BG, Lipt åk BG. Instrument engineers' handbook: Process control and optimization. CRC; 2005.

11. Step Motor. <http://www.amci.com/tutorials/tutorials-stepper-vs-servo.asp>. Accessed 2014 5 July.

12. Flexcell International Corporation. 2011 Flexcell® FX-5000TM Tension System<http://www.flexcellint.com/slideshow2.htm>. Accessed 2011 10/06.

13. Stephen P. Arold, Joycey. Wong and Bela Suki. Design of a New Stretching Apparatus

and the Effects of Cyclic Strain and Substratum on Mouse Lung Epithelial-12 Cells. Ann of Biomedical Engineering, 2007 07; 35 (7): 1156–1164.

14. William J. Richardson, Richard P. Metz, Michael R. Moreno, Emily Wilson and James E. Moore, Jr. A Device to Study the Effects of Stretch Gradients on Cell Behavior. J Biomech 2011; 133 (101008): 1-9.

15. Daniel L. Feeback, Mark S. F. Clarke, "Uni-directional cell stretching device," U.S.Patent 6,107,018, Aug, 02, 2000.

16. Park JS, Chu JSF, Cheng C, Chen F, Chen D, Li S. Differential effects of equiaxial and uniaxial strain on mesenchymal stem cells. Biotechnol Bioeng 2004; 88 (3):359-68.

17. William Campbell, Michael Howard, Jarrett Shamlian. Equi-biaxial Stretcher of a Thin Membrane <http://www.mie.neu.edu/sites/default/files/pdfs/mie/Capstone/Mechanical_Engineering/ME_2012_04_Equi-biax.pdf>. Accessed 2014/06/15.

18. Alan R. Shapiro, Martha L. Gray, Luis A. Melendez, Jonathan L. Schaffer, John D. Wright, Jose G. Venegas, "Cell stretching apparatus," U.S.Patent 5,217,899, Aug, 24, 1990.

19. Brent Duoba, Joseph Lombardo, Kyaw Thu Minn, Juan Rodriguez, "Device to Dynamically Stretch Cells during Microscopic Visualization", B.S.project, Worcester Polytechnic Institute, MA, 2012.

VITA

The author was born in China in 1989. He was awarded bachelor degree with honor in South China University of Technology (SCUT), Guangzhou, China in June 2012. After that, he attended Lehigh University pursuing a Master of Science degree supervised by Professor Yaling Liu. Then he attends the lab to have research about design of cell stretching device.